END

MICROCOPY RESOLUTION TEST CHART
NATIONAL BUREAU OF STANDARDS-1963-A

YALE UNIVERSITY

MECHANICAL ENGINEERING

⑫

1984 Annual Report

PROPERTIES OF MATERIALS USING ACOUSTIC WAVES

N00014-76-C-0527

P.I. - R.E. Apfel

DTIC
ELECTE
FEB 20 1985

S D

B

October 1984

Approved for public release; distribution unlimited.

SECURITY CLASSIFICATION OF THIS PAGE (When Data Entered)

REPORT DOCUMENTATION PAGE		READ INSTRUCTIONS BEFORE COMPLETING FORM
1. REPORT NUMBER	2. GOVT ACCESSION NO. A150 465	3. RECIPIENT'S CATALOG NUMBER
4. TITLE (and Subtitle) PROPERTIES OF MATERIALS USING ACOUSTIC WAVES		5. TYPE OF REPORT & PERIOD COVERED Annual Nov. 1, 1983–Oct. 31, 1984
		6. PERFORMING ORG. REPORT NUMBER
7. AUTHOR(s) R.E. Apfel		8. CONTRACT OR GRANT NUMBER(s) N00014-76-C-0527
9. PERFORMING ORGANIZATION NAME AND ADDRESS Dept. of Mechanical Engineering, Yale University P.O. Box 2159, 9 Hillhouse Ave., New Haven, CT 06520		10. PROGRAM ELEMENT, PROJECT, TASK AREA & WORK UNIT NUMBERS 61153N (Prog.El.#) RR011-08-01(Proj.Task Area#) NR 384-701(Work Unit #)
11. CONTROLLING OFFICE NAME AND ADDRESS Office of Naval Research Physics Division Office (Code 412) Arlington, VA 22217		12. REPORT DATE October 1984
		13. NUMBER OF PAGES 83
14. MONITORING AGENCY NAME & ADDRESS(if different from Controlling Office)		15. SECURITY CLASS. (of this report) Unclassified
		15a. DECLASSIFICATION/DOWNGRADING SCHEDULE

16. DISTRIBUTION STATEMENT (of this Report)

Approved for public release; distribution unlimited

17. DISTRIBUTION STATEMENT (of the abstract entered in Block 20, if different from Report)

18. SUPPLEMENTARY NOTES

19. KEY WORDS (Continue on reverse side if necessary and identify by block number)

Interfacial tension, radiation pressure, nonlinear acoustics, acoustic
levitation, acoustic cavitation, calibration

20. ABSTRACT (Continue on reverse side if necessary and identify by block number)

Our goal of characterizing materials using acoustic waves was forwarded
through a number of projects: 1) We have refined our modulated radiation pres-
sure technique for characterizing the interfaces between liquids so that we can
automatically track changes in interfacial tension over time due to contaminants,
surfactants, etc. 2) We have improved and simplified our acoustic scattering
apparatus for measuring distributions of the properties of microparticle samples,
which will allow us to distinguish particulates in liquids by size, compressi-
bility, and density. 3) We are continuing our work on theoretical approaches

DD FORM 1473 EDITION OF 1 NOV 65 IS OBSOLETE
1 JAN 73
S/N 0102-LF-014-6601

SECURITY CLASSIFICATION OF THIS PAGE (When Data Entered)

to nonlinear acoustics which should permit us to cast problems with geometric and other complexities into a manageable form. 4) Our studies of cavitation have enabled us to derive an analytic expression which predicts the acoustic pressure threshold for cavitation at the micrometer scale — where surface tension effects are important. This work has relevance to the consideration of possible bioeffects from diagnostic ultrasound. 5) Other projects include the calibration of hydrophones using acoustically levitated samples, and the investigation of solitary waves of the sort discovered by Wu, Keolian and Rudnick (Phys. Rev. Letters 52, 1421 (1984)). These relatively new studies are discussed in the renewal proposal.

ABSTRACT

· Our goal of characterizing materials using acoustic waves was forwarded through a number of projects: 1) We have refined our modulated radiation pressure technique for characterizing the interfaces between liquids so that we can automatically track changes in interfacial tension over time due to contaminants, surfactants, etc. 2) We have improved and simplified our acoustic scattering apparatus for measuring distributions of the properties of microparticle samples, which will allow us to distinguish particulates in liquids by size, compressibility, and density. 3) We are continuing our work on theoretical approaches to nonlinear acoustics which should permit us to cast problems with geometric and other complexities into a manageable form. 4) Our studies of cavitation have enabled us to derive an analytic expression which predicts the acoustic pressure threshold for cavitation at the micrometer scale — where surface tension effects are important. This work has relevance to the consideration of possible bioeffects from diagnostic ultrasound. 5) Other projects include the calibration of hydrophones using acoustically levitated samples, and the investigation of solitary waves of the sort discovered by Wu, Keolian and Rudnick. (Phys. Rev. Letters 52, 1421 (1984)). These relatively new studies are discussed in the renewal proposal.

A-1

INTRODUCTION

Below, we present a summary of our current activities and progress in the past year. We stress the most recent progress, leaving to journal publications (see PUBLICATIONS....) the details of published work.

1. Characterizing interfaces using modulated acoustic radiation pressure. (Dr. Hsu, R. Agostinelli, R. Apfel)

The work reported in the Ph.D. thesis of Mr. C.-J. Hsu describes the measurement and analysis of the interfacial tension of superheated hydrocarbons with water. As an example, liquid propane at room temperature and atmospheric pressure is superheated by 70 degrees C. When acoustically levitated in water and set into quadrupole oscillations, we have been able to deduce the interfacial tension of superheated propane drops with water. We noticed that this interfacial tension changes with time owing to the partial solubility of propane with water.

We decided that it would be desirable to track automatically changes in the interfacial tension with time, not only for the propane case but also for cases in which contaminants or surfactants are present in the water or oil phase. Our measurement procedure is particularly well suited to this change. Figure 1 displays the set-up in which the phase of the driving signal is compared with that of the drop response, as measured optically, as the drop undergoes quadrupole shape oscillations. By adjusting the frequencies of one of the oscillators in the set-up, we can produce a 90° phase shift between driving signal and response, which corresponds closely to the resonance condition. As figure 1 illustrates, a Lock-In amplifier provides an "error" signal if the phase is other than

90°, and this error signal will correct the frequency of the appropriate voltage-controlled oscillator in order to restore the 90° phase condition for resonance. From a plot of the frequency with time we can directly deduce the interfacial tension with time.

For example, a copy of the data is given in Figure 2. At time $t = 0$ a small amount of concentrated surfactant is introduced at the surface of the water. It takes about 5 minutes for this surfactant to diffuse through the water to the levitated hexane drop. Then the interfacial tension drops rapidly. The rate at which it drops is an indication of the rate at which surfactant molecules are being added to the drop surface. Eventually, after 90 minutes, equilibrium is reached.

In addition to tracking the quadrupole resonance, we have also added a feedback circuit to keep the acoustic levitation system in resonance, since the resonance frequency can change with changes in temperature and in the height of the water column in which the oil drop is suspended.

The apparatus, as it now stands, is a powerful tool for characterizing the interfacial tension of immisible liquid systems in a variety of circumstances, including changes with time of surfactant concentration, temperature (see Renewal proposal), etc.

2. Analysis of surface oscillations in order to characterize the inter-
    layer. (Dr. Hsu and R. Apfel)

Dr. Hsu has developed a theoretical formulation for the motion of the viscous fluid in and around a drop undergoing quadrupole shape oscillations. This formulation is not an exact approach, as with the work of Marston, but is rather an ad hoc approach that bares the physical nature

of the process. In addition, it provides a way of dealing with geometries other than the few that can be dealt with exactly. Moreover, we have been able to handle cases in which the surface is contaminated with an interfacial layer. The ad hoc approach allows one to characterize this interface with an "interfacial viscosity". By measuring damping constants with and without contaminants we may be able to quantify this interfacial property. This recent work is described more fully in a paper entitled "Quadrupole Oscillations of Drops for the Determination of Interfacial Tension", by Dr. C.-J. Hsu which is submitted with this Annual Report.

3. Microparticle characterization using acoustic scattering.
   (M. Roos, C.-J. Hsu, and R. Roy)

We have been using 30 MHz tone bursts to scatter off microparticles as they individually fall through the acoustical focal region of the transmitter. We receive the scattered signal at two angles which permits us to characterize the particles by compressibility and density if we know the size.

The National Institutes of Health are the primary supporters of this work, especially with regard to the characterization of biological cells. Some equipment for this work has been purchased on this ONR contract. The work of interest to our present contact resides in our desire to discriminate between different types of microparticles. For instance, in an oil sample, one would not be able to distinguish between an oil drop or an aluminum wear particle if one received a single scattered signal. But with two scattered signals (at 90° and 180°) we can differentiate between

rigid and compressible samples.

Recent changes in the apparatus have resulted in a simpler system. We have reduced the number of transducers from three to two by using the transmitter as a backscatter receiver (which must, therefore, have a 100 dB dynamic range). And we have moved most of the signal processing from software to hardware allowing for almost instantaneous microparticle characterization. (This work is described in two articles which are now in draft form, and which will be sent to ONR when completed.)

4. Micro-cavitation (R. Apfel).

A bubble of radius R_0 containing gas of specific heats ratio, γ, exists in a liquid of density ρ, viscosity μ, surface tension (with a gas) of σ. The ambient pressure and temperature are P_0 and T_0 respectively. The bubble is subjected to a single acoustic cycle, period τ (corresponding to a frequency f). For what acoustic pressure amplitude, P_A, will the bubble grow and collapse, with the internal temperature of the bubble reaching a maximum temperature in the range of 2500-5000 °K? We have found an approximate analytic expression that answers this question. Writing $p \equiv P_A/P_0$, the expression is written more easily in the form of the acoustic frequency f as a function of p, the liquid parameters, and the state of the liquid.

$$f = \frac{\frac{1}{3\pi R_0}\sqrt{\frac{P_0(p-1)}{\rho}}\left[\sqrt{\frac{2(p-1)}{p}} + \sqrt{\frac{2(p-p_b)}{p}}\right]}{\left[\frac{T'/(\gamma-1)T_0}{1 + \frac{2}{3}(p-1)}\right]^{1/3} + \frac{8\mu}{3R_0}\sqrt{\rho\frac{1}{P_0(p-1)}} - 0.46}$$

In this expression, p_b, the "Blake threshold," is given by:

$$p_b = 1 + \frac{4}{9} X_B \sqrt{\frac{3X_B}{4(1+X_B)}} \,,$$

where $\quad X_B \equiv \dfrac{2\sigma}{R_o P_o}$.

Also T' is the maximum internal bubble temperature.

For T' much above a few thousand °K, the above expression breaks down badly, with heat conduction effects becoming very important. For bio-effects, however, we expect that significant free-radical formation will occur for T' < 3000°K (T.K. Sakena and W.L. Nyborg, J. Chem. Phys. 53, 1722 (1970)).

We have compared our analytical results with numerical ones of Flynn (J. Acoust. Soc. Am. 72, 1926 (1982)) and find that the agreement is fairly reasonable.

Our analytical results may be of some use in trying to assess the likelihood of bioeffects due to cavitation under conditions of diagnostic ultrasound. Moreover, they may also be applicable when trying to assess the effects of high frequency ultrasound on the kinetics of chemical reactions.

5. New theoretical approaches in nonlinear acoustics
   (R.M. McGowan and Professor B.-T. Chu)

We are working to solve for steady second order quantities, radiation pressure and streaming, in the limit of small body dimension-to-wavelength ratio. This involves solving the first order, or linear,

scattering problem, under sufficient restrictions on acoustic amplitude,
so that the near-field is known. A good way to solve scattering problems
is with the method of matched asymptotic expansions. This method will
provide the necessary information of the near-field around objects of a
variety of shapes. Often, it is possible to use conformal mapping since
the near-field is incompressible to some approximation. Since steady
streaming relies on the dissipation of acoustic energy, which is strong-
est near boundaries, a viscous boundary layer theory for steady second
order quantities is developed. The boundary layer theory helps us dis-
tinguish the quantities important for steady radiation pressure and
those important for streaming.

We have non-dimensionalized the equations of motion and set restric-
tions on the relative sizes of the parameters. The parameters of interest
are body dimension/wavelength, fluid particle amplitude/wavelength, Stokes
layer thickness/body dimension, and Prandtl number. Scaling is done to
distinguish the far-field from the near-field, which in turn is distin-
guished from the viscous boundary layer. We write the perturbation equa-
tions to higher orders in the perturbation parameters in the different
regions. Some useful information comes from these equations, such as
the decoupling of the radiation pressures problem from the steady stream-
ing problem in the viscous boundary layer. Examples include calculation
of steady streaming over a smooth wedge due to an incident plane wave,
the effect of curvature of the incident wave on radiation pressure, and
the effect of a viscous boundary layer on the radiation pressure on a
sphere.

We are looking at the interaction of an imposed steady field with steady second order acoustic quantities (especially steady streaming). We want to see whether important alterations to the imposed steady field are made, such as the shape of a boundary layer or rate of heat conduction. The approach is an extension of the work discussed above, since steady mean field changes are assumed to occur on a scale much smaller than the wavelength.

Consider, for example, a channel flow with steady boundary layer that is thin compared to the width of the channel, and a "plane wave" with wavelength greater than the width of channel, but with a Stokes layer much thinner than the steady boundary layer. The main effect of this channel flow on the steady streaming is to focus the first order acoustic energy toward the walls and thus increase the streaming. We are also working on the effects of a steady temperature gradient.

RELEVANT PUBLICATIONS AND MANUSCRIPTS SUBMITTED SINCE 1 Oct. 1983

M. A. H. Weiser, R.E. Apfel, and E.A. Neppiras, "Interparticle forces on red
cells in a standing wave field," Acustica (in press).

C.-J. Hsu, "Interfacial Tension Between Water and Selected Superheated
Liquids by Quadrupole Oscillations of Drops," Ph.D. Thesis,
Yale University, Dec. 1983.

R.E. Apfel, "The effective nonlinearity parameter for immiscible liquid
mixtures," J. Acoust. Soc. Am. 74, p.1866, 1983.

Z. Zhu, M.S. Roos, W.N. Cobb and K. Jensen, "Determination of the acoustic
nonlinearity parameter B/A from phase measurements," J. Acoust.
Soc. Am. 74, p.1518, 1983.

B.-T. Chu and R.E. Apfel, "Are acoustic intensity and potential energy
density first- or second order quantities?," Am. J. Phys. 51,
p.916, 1983

B.-T. Chu and R.E. Apfel,"Response to the Comments of Nyborg and Rooney
[J. Acoust. Soc. Am. 75, 263-264 (1984)]," J. Acoust. Soc. Am.
75, p.1003, 1984.

R.E. Apfel, "Acoustic cavitation series: part four, Acoustic cavitation
inception," Ultrasonics, 22, p.167, 1984.

Yale University

DEPARTMENT OF MECHANICAL ENGINEERING

Mason Laboratory
P.O. Box 2159 Yale Station
New Haven, Connecticut 06520

(203) 436-8674

1 August 1984

Dr. Logan E. Hargrove
Office of Naval Research
Physics Division
Code 412
800 N. Quincey Street
Arlington, VA 22217

Dear Dr. Hargrove:

This letter represents the mid-year Status Report on the activities of Contract N00014-76-C-0527.

Current Personnel:

Paid:

1) R.E. Apfel - Principal Investigator

2) Dr. Chaur-Jian Hsu - Postdoctoral Associate. He has received his Ph.D. in November 1983 based on work supported by ONR. He has just received his permanent resident status.

3) Mr. Richard McGowan - Assistant in Research (3rd year graduate student).

4) Mr. Christopher Mansfield - Apprentice in DOD Science and Engineering Apprenticeship Program for High School Students

5) Mr. Raymond Agostinelli - participant in our Yale Summer Research Program. (He is going into his senior year at Dartmouth in the fall.)

Unpaid:

1) Professor B.-T. Chu, who acts as an adviser to Mr. McGowan and who works on theoretical aspects of our problems.

2) Mr. Ronald Roy - an ONR fellow - working on microparticle characterization. He has finished his first year as a Ph.D. graduate student.

Scientific Progress:

Scientific progress has been in the following areas:

1) Apparatus for microparticle characterization (Dr. Hsu, Mr. Roy, R. Apfel): tone bursts at 30 MHz scattered from micron-scale particles allow for the characterization of these particles by size, compressibility, and density. Major modifications to the apparatus include: reducing the number of transducers from three to two by using the transmitted as a backscatter receiver;

taking most of the processing that was done in software and performing it in new hardware, thereby allowing for almost instantaneous information on the particle's properties as it passes the focal zone of the transducer.

2) Automatic tracking of changes in interfacial tension (Dr. Hsu, Mr. Agostinelli, R. Apfel).

When a drop of oil is placed in an aqueous solution containing a surfactant, the interfacial tension may drop from 50 dynes/cm to 5 dynes/cm over a period of an hour. We have added a phase locked loop to our system which uses modulated acoustic radiation pressure to measure interfacial tension so that now the interfacial tension is automatically tracked in time. (see Appendix A)

3) Some problems in steady second order acoustics (Mr. McGowan, and Dr. Chu).

    See Appendix B

4) Other problems being worked on are:

    a) Analytic predictions of cavitation in the megahertz range (R. Apfel)

    b) Measurements of B/A using a newly acquired Microultrasonic Interferometer. (R. Apfel)

Other Research Support:

NIH - Cell Characterization and Deformation with Ultrasound
    Annual Amount $59,000 (direct costs).

DOE - Neutron Detection Using Superheated Drops
    Annual Amount $86,000.

Current Status of Contract Funds:

Spending on the presented ONR contract is proceeding as budgeted and we anticipate no unexpended funds at the end of the contract period.
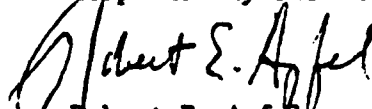
Equipment Purchases thus far during contract year:

ONR has contributed 50% ($4225) to the purchase of a PLR-1000 Ultrasonic Interferometer from MicroUltrasonics, Inc.

External Communications (since Feb. 1, 1984):

1. R. Apfel, "Acoustic Cavitation Inception," Ultrasonics (GB) 22(4), 167 (July 1984).

2. M.A. Weiser, R. Apfel, and E.A. Neppiras, "Interparticle forces on red cells in a standing wave field," Acustica, in press.

Respectfully submitted,

Robert E. Apfel

Attachments

cc: Mr. Fred E. Walters
     ONR Administrative Rep. - N.Y.

MODEL FOR THE QUADRUPOLE OSCILLATIONS OF DROPS FOR DETERMINING INTERFACIAL TENSION

Chaur-Jian Hsu and Robert. E. Apfel

Yale University

1984

A simplified model is developed for describing the free and forced oscillations of the quadrupole mode of a liquid drop freely suspended in a liquid host. The damping rate of the free oscillations and the phase-frequency relation for the forced oscillations are derived and compared with previous theories. A parameter, the interfacial viscosity, is included as an example to demonstrate the versatility of this simplified model. The application of this model in determining the interfacial tension between two liquids is discussed. The experimental technique and some results for different liquids are briefly reviewed.

1. INTRODUCTION

Free and forced oscillations of drops and bubbles in another fluid have long been interesting subjects in various scientific and engineering problems. Later in this article, we will discuss some applications of measuring the interfacial tension between two liquids. Rayleigh gave the derivation for the small oscillations of a liquid mass about its spherical equilibrium shape. Lamb generalized the problem by supposing that the liquid drop was surrounded by an infinite mass of another liquid. The liquids were assumed inviscid by both authors so that viscosity did not enter their expressions for the oscillation frequency. Lamb also discussed the effect of small viscosity on the small oscillations of a liquid drop (no surrounding liquid), or a spherical bubble in a liquid. Miller and Scriven (1968) did an analysis of small oscillations of a viscous fluid droplet immersed in another viscous fluid. The frequency and rate of damping of _free_ oscillations were derived for arbitrary values of the physical properties of the fluids as well as interfacial viscosity and elasticity coefficients. Marston (1980) independently derived the same general results for free oscillations, and found a new term to correct the decay time. The phase-frequency relation for _forced_ oscillation was also established for the first time in this work of Marston. In this paper, we will present a simplified model to describe the oscillations of a drop in another fluid. The damping of free oscillations and the phase-frequency relation of forced oscillations are derived based on this model and will be compared with the previous theories derived in a direct mathematical

approach. This model, developed in an ad hoc manner, may have special advantages in some situations. For example, if the equilibrium shape of the drop is non-spherical, or when the interface exhibits some elastic or viscous characteristics different from the two fluids.

2.   COMPARISON WITH THE MASS-SPRING SYSTEM

Although the motion of the shape oscillations of a drop in a host fluid in a certain mode is three-dimensional, there is only one degree of freedom. The analogy between the oscillations of a drop and the oscillations of a basic mass-spring system is obvious by comparing the following two equations. It is this analogy that lead to the idea of this simplified model. For a system of mass m and stiffness k, the natural frequency is

$$\omega = (k/m)^{\frac{1}{2}}. \tag{1}$$

For the free oscillation of a drop-host system without damping, the natural frequency, for the quadrupole mode, is (Lamb)

$$\omega^* = \left[\frac{24\sigma}{R^3(3\rho_i + 2\rho_o)} \right]^{\frac{1}{2}}. \tag{2}$$

where ω^* is the angular frequency, n is the mode, σ is the interfacial tension which provides the stiffness, ρ_i and ρ_o are the densities of the inner (drop) and outer (host) liquid respectively, and R is the mean radius of the drop.

However, if the resistive force is considered, these two systems show an important difference. When the mass-spring system is subject to

- 3 -

a resistive force, which is normally assumed proportional to velocity, and is driven by a force $F_0\cos(\omega t)$, the equation of motion is:

$$m\frac{d^2x}{dt^2} + b\frac{dx}{dt} + kx = F_0\cos\omega t. \tag{3}$$

The resonance frequency, if we define it as the frequency with 90^0 phase angle, has the same form as that given in Eq. (1). Notice that the damping term b does not appear in this expression. Fig. 1 shows a schematic diagram for the impedance to the driving force of this system. The component due to damping, $j\omega b$, has a phase angle of 90^0; this fact is responsible for the resonance frequency, $\omega(90^0)$, being independent of the damping coefficient b. On the other hand, when the viscosity of the two fluids is non-negligible, due to the nature of the viscous damping in liquids, the impedance due to viscosity has a component whose phase is not 90^0. Therefore, the resonance frequency $\omega(90^0)$ is no longer the same as the ω^* in Eq. (2). The $\omega(90^0)$ is not only a function of stiffness and mass, but also a function of viscosity,

$$\omega(90^0) = \text{function } (\sigma, \rho, R, \text{viscosity}).$$

It is our primary goal in this work to derive the above function.

3.   VELOCITY DISTRIBUTION

The two bulk fluids are assumed to be isothermal, incompressible, and Newtonian. The drop is assumed freely suspended and its equilibrium shape can be taken as spherical. For the driving force, acoustic radiation pressure in our experiment, we assume its tangential component on the interface is much smaller than the normal component.

For simplicity, all the following expressions are for oscillations in the quadrupole mode only. Nevertheless, the method can be applied similarly to other modes. Spherical coordinates with polar angle θ and radius r are used to describe the motion. Due to the symmetry with respect to the vertical axis through the center of the spherical drop, expressions are independent of the azimuthal angle.

3.1 Inviscid Drop in an Inviscid Host

For small quadrupole oscillation about a spherical form, the radial position of the interface, r, at any instant may be given as (Lamb) (Rayleigh):

$$r = R_0 + \varepsilon Y_2(\theta)\sin(\omega t). \tag{4}$$

where

r = the radial position of the interface relative to the center of the equilibrium sphere,

R = the equilibrium radius,

R_0 = a value close to but not equal to the equilibrium radius R

$$= R \left[1 + \frac{4\varepsilon^2}{5R^2} \right]^{-1}, \tag{5}$$

ε = the amplitude of the oscillation,

ω = the angular frequency,

$Y_2(\theta)$= spherical harmonic function of order 2

$= 3\cos^2\theta - 1.$

Assuming the flow is inviscid, we have the velocity potential which is determined by the boundary condition in Eq. (4), at the internal points (Lamb),

$$\phi_i = - \frac{\omega R}{2} \frac{r^2}{R^2} \varepsilon \, Y_2(\theta) \cos(\omega t) \, , \qquad (6)$$

and, at the external points,

$$\phi_o = \frac{\omega R}{3} \frac{R^3}{r^3} \varepsilon \, Y_2(\theta) \cos(\omega t) \, , \qquad (7)$$

We use subscripts i and o to denote the terms related to the inner (drop) and the outer (host) flow, respectively.

The corresponding velocity distribution is readily obtained from the velocity potential,

$$u = u_r e_r + u_\theta e_\theta = -\nabla \phi \, , \qquad (8)$$

where the subscripts r and θ denote the components in the direction of r and θ respectively. From Eqs. (6), (7), and (8), the radial and tangential component of the flow velocity in the inner and outer region are:

$$u_{ri} = (1/R)\varepsilon \omega r(3\cos^2\theta - 1)\cos(\omega t) \, , \qquad (9)$$

$$u_{\theta i} = (-3/2R)\varepsilon \omega r \sin(2\theta)\cos(\omega t) \, , \qquad (10)$$

$$u_{ro} = (R/r)^4 \varepsilon \omega (3\cos^2\theta - 1)\cos(\omega t) \, , \text{ and} \qquad (11)$$

$$u_{\theta o} = (R/r)^4 \varepsilon \omega \sin(2\theta)\cos(\omega t) \, . \qquad (12)$$

Fig. 2 shows a schematic diagram of the streamlines at a certain instant when the drop is moving from a spherical shape toward a prolate shape.

For small enough amplitude ε, the velocity at the interface may be considered as the value of the above functions evaluated at r=R. Notice that the radial velocity is continuous across the interface as expected,

$$\frac{\partial r}{\partial t}\bigg|_{r=R} = U_{ri} = U_{ro} = \varepsilon\omega(3\cos^2\theta-1)\cos(\omega t) ,\qquad (13)$$

where U_{ri} and U_{ro} are the values of u_{ri} and u_{ro} evaluated at r=R respectively. But the tangential velocities at the two sides of the interface are <u>opposite</u> in direction and have their magnitudes related as:

$$U_{\theta i} = - (3/2)U_{\theta o} \qquad (14)$$
$$= - (3/2)\varepsilon\omega\sin(2\theta)\cos(\omega t) ,$$

where $U_{\theta i}$ and $U_{\theta o}$ are the values of $u_{\theta i}$ and $u_{\theta o}$ evaluated at r=R respectively.

3.2   A Modified Velocity Distribution with Small Viscosity

The velocity distribution predicted by the velocity potential of inviscid flow, as shown in Fig. 2, is found to agree with the outcome of a qualitative photographic study done by Trinh, Zwern, and Wang (1982). On the other hand, the discontinuity of the tangential velocity across the interface can not be true physically. This velocity "jump" has to be smoothed out by viscosity.

We assume the viscosities of both inner and outer fluid are small, so that the boundary layer thickness (or viscous wavelength) at each side of the interface is smaller than, say, 1/10 of the radius of the

- 7 -

drop. Then we may model the flow distribution in an ad hoc way by combining a thin boundary layer at each side of the interface with the potential flow, derived on the inviscid assumption, at all points other than the boundary layer. Based on this approximate flow distribution, we compute the damping rate and the phase-frequency relation.

To consider the flow in the boundary layer around the interface, we take a rather simple approach. We first estimate the tangential velocity of the interface, u_s, and then consider the boundary layer at each side of the interface separately as a consequence of an enforced oscillation of a solid boundary.

3.2.1 Tangential Component of the Interfacial Velocity

If we assume that there is no pure rotation associated with this oscillation, then the interface should oscillate in phase with the potential flow, as does u_s--the tangential component of the velocity of the interface. Physically, we know that the velocity u_s must be in between $u_{\theta i}$ and $u_{\theta o}$. The ratio of the amplitudes $U_s/U_{\theta i}$ or $U_s/U_{\theta o}$ should be determined by the following two factors: 1) The momentum carried by the "external stream", which is a function of the density and velocity. 2) The diffusivity of momentum, that is, the viscosity.

We assume that for the tangential velocity in the boundary layer the gradient in radial direction is much greater than the gradient in tangential direction. In other words, the boundary layer thickness is

- 8 -

much smaller than, say, a quarter of the circumference of the space. Then, locally, we may approximate the flow in the boundary layer as a stream of viscous, incompressible fluid over a parallel stream of different density and viscosity. Also, to a first approximation, we may use $U_{\theta i}$ and $U_{\theta o}$ as the "external stream velocities". Under these approximation, the results of the work " The Velocity Distribution in the Laminar Boundary Layer between Parallel Stream" done by Lock (1951) can be applied to compute the U_s as follows:

$$c \equiv \frac{U_s}{U_{\theta i}} = \frac{\lambda + (\delta/\mu)}{1 + (\delta/\mu)} , \tag{15}$$

$$\frac{\delta}{\mu} = \left[\frac{1.425\lambda + 0.858}{2.283\lambda\rho\mu} \right]^{\frac{1}{2}} , \tag{16}$$

where $\lambda = \dfrac{U_{\theta o}}{U_{\theta i}} = -\dfrac{2}{3}$ (see Eq. (14)), $\quad \delta = \dfrac{\delta_o}{\delta_i}, \quad \rho = \dfrac{\rho_o}{\rho_i}, \quad \mu = \dfrac{\mu_o}{\mu_i} ,$

δ denotes boundary layer thickness, ρ denotes density, and μ denotes dynamic viscosity. With a given u_s, the boundary layer at each side of the interface can be modeled as the flow over an oscillating boundary at the velocity of $u_s - u_{\theta i}$ and $u_s - u_{\theta o}$, as described below.

4. DAMPING OF FREE OSCILLATION

Now we discuss the damping rate of the free oscillation of a drop immersed in another fluid, making use of the flow distribution described above. The resultant damping rate is expressed in terms of known parameters including the inner and outer density, ρ_i and ρ_o ; the inner

- 9 -

and outer viscosity, μ_i and μ_o ; the radius of the drop R; and the
oscillation frequency ω. The result will be used in the derivation of
phase-frequency relation for forced oscillations.

The damping rate is governed by the following relation:

$$\frac{d}{dt} \text{(total energy)} = \text{(rate of dissipation)} .$$

In the problem of an oscillatory drop in a host, the total energy T.E.
is the sum of the instantaneous potential energy P.E. and kinetic energy
K.E. The potential energy is a function of the interfacial tension, and
the change of the interfacial area. The kinetic energy is a function of
the density and the flow distribution. The energy dissipation is due to
the viscous dissipation in the boundary layer near the interface and in
the potential flow at the other points.

The viscous dissipation may be considered as the sum of the
following four parts:
1) the dissipation in the inner irrotational flow,
2) the dissipation in the outer irrotational flow,
3) the dissipation in the inner boundary layer, and
4) the dissipation in the outer boundary layer.
They are derived separately as follows.

The dissipation in a spherical mass of fluid with radius r,
calculated on the assumption that the motion is irrotational, is, by
art. 355 of (Lamb),

- 10 -

$$\mu \iint \frac{\partial u^2}{\partial r} r^2 d\Omega = \mu r^2 \frac{\partial}{\partial r} \iint u^2 d\Omega \ , \tag{17}$$

where $u^2 = u_r^2 + u_\theta^2$, Ω denotes the solid angle, and $d\Omega = 2\pi \sin\theta d\theta$. The following relation can be applied,

$$\iint u^2 d\Omega = \frac{1}{r^2} \frac{\partial}{\partial r} \iint \phi \frac{\partial \phi}{\partial r} r^2 d\Omega \ . \tag{18}$$

We evaluate the result at $r=R$, and take the time average over one period $2\pi/\omega$. We obtain:

$$\frac{\omega}{2\pi} \int_{t=0}^{2\pi/\omega} \mu \int \frac{\partial u^2}{\partial r} r^2 d\Omega = 8\pi\mu_i \varepsilon^2 R\omega^2 \ . \tag{19}$$

The above expression gives the dissipation in the irrotational flow in the drop, on the assumption that the amplitude of oscillation and the boundary layer thickness are much smaller than the radius of the drop.

The same method can be applied to give the time averaged rate of dissipation in the irrotational flow outside the drop:

$$(64/3)\pi\mu_o \varepsilon^2 R\omega^2 \ . \tag{20}$$

In an oscillatory boundary layer, the time average, over one cycle, of the rate of dissipation in the boundary layer per unit area of the surface (boundary) is (Batchelor)

$$\frac{\mu U^2}{2\delta} \ , \tag{21}$$

where U is the amplitude of the oscillatory velocity of the irrotational flow outside the boundary layer (external stream velocity), and δ is the

boundary layer thickness. We approximate the boundary layer thickness

as: $\delta = (2\nu/\omega)^{\frac{1}{2}}$ (Batchelor). Suppose the boundary layer thickness is
much smaller than the radius of the drop, so that Eq. (21) is applicable
and the amplitude of the "external stream velocity" may be approximated
by $U_{\theta i} - U_s$. U_s is the amplitude of the tangential velocity of the
interface and $U_s = cU_{\theta i}$ (see Eq. (15)). On making use of Eqs. (10), (15),
and (21), integrating over the interface $r=R$, we have the rate of
dissipation in the inner boundary layer as:

$$\iint \frac{\mu(1-c)^2[(3/2)\varepsilon\omega\sin(2\theta)]^2}{2(2\nu_i/\omega)^{\frac{1}{2}}} dA = \frac{12\pi(1-c)^2\mu_i\varepsilon^2R^2\omega^{5/2}}{5(2\nu_i)^{\frac{1}{2}}} . \tag{22}$$

Applying the same argument to the outer boundary layer with the
amplitude of the external stream velocity $U_{\theta o} - U_s$, we obtain the time
averaged rate of dissipation in the outer boundary layer

$$\iint \frac{\mu_o(1+1.5c)^2\varepsilon^2\omega^2(\sin2\theta)^2}{2(2\nu_i/\omega)^{\frac{1}{2}}} dA = \frac{16\pi(1+1.5c)^2\mu_o\varepsilon^2R^2\omega^{5/2}}{15(2\nu_o)^{\frac{1}{2}}} . \tag{23}$$

4.1   The Total Energy of the Oscillation

The kinetic energy of this drop-host system reaches its maximum value,
while the potential energy is (set) zero (see section 5.1), at, say, $t=0$
in Eq. (4). We take this maximum kinetic energy as the total energy

$$K.E. = \tfrac{1}{2}\rho \iint \phi \mathbf{u} \cdot \mathbf{n} dA$$

$$= \tfrac{1}{2}\rho \iint \phi u_r dA .$$

Assuming that the interface is approximated by $r=R$, and employing the
irrotational velocity distribution, we have

$$K.E.)_{inner,max} = (4/5)\pi\varepsilon^2R^3\rho_i\omega^2 . \tag{24}$$

Similarly, we have

$$\text{K.E.})_{outer,max} = (8/15)\pi\varepsilon^2 R^3 \rho_o \omega^2 \quad . \tag{25}$$

Therefore, the total energy is

$$\text{T.E.}) = (4/15)\pi\varepsilon^2 R^3 (3\rho_i + 2\rho_o)\omega^2 \quad . \tag{26}$$

4.2 Damping Constant

If the total energy T.E. $= x\varepsilon^2$, and the rate of dissipation is $y\varepsilon^2$, where ε represents the amplitude at the time t, and if we define damping constant S in such a way that $\varepsilon = \varepsilon_0 e^{-tS}$ then

$$S = (\tfrac{1}{2})(y/x) \quad . \tag{27}$$

By using the total energy and the rate of dissipation obtained above, together with the above equation, we have the damping constant S as:

$$S = S_b + S_i + S_o \quad , \tag{28}$$

where

$$S_b = \frac{(2\omega)^{\frac{1}{2}}}{R\Gamma} \; [2.25(1-c)^2(\mu_i\rho_i)^{\frac{1}{2}} + (1+1.5c)^2(\mu_o\rho_o)^{\frac{1}{2}}],$$

$$S_i = \frac{15\mu_i}{R^2\Gamma} \quad ,$$

$$S_o = \frac{40\mu_o}{R^2\Gamma} \quad ,$$

$$\Gamma = 3\rho_i + 2\rho_o ,$$

- 13 -

where the subscripts b denotes the contribution of dissipation from the boundary layer, i denotes the contribution from the inner irrotational flow, and o denotes the contribution from the outer irrotational flow. Lamb derived the damping for the oscillations of a liquid sphere in air and the damping for the oscillations of a gas bubble in liquid, as the above S_i and S_o.

4.3 Examples and Comparison with the Previous Theories

We take three examples to illustrate the calculation and to compare the results with that obtained by previous theories and with one set of experimental data from previous work.

1) For an air bubble of radius 0.1 cm in water, $\rho_i = 0.0012$ g/cm^3, $\mu_i = 0.018$ cp, $\rho_o = 0.997$ g/cm^3, $\mu_o = 0.894$ cp, $\sigma = 72$ dyne/cm.

(a) By Marston's theory (1980, table 1 and 2):

$$s = 18.35 \text{ 1/sec} .$$

(b) By Lamb's formula,

$$s = 17.94 \text{ 1/sec} .$$

(c) By this simplified model:

$$\omega/2\pi = 147.9 \text{ Hz (a given value)}$$

$$S = S_b + S_i + S_o$$
$$= 0.627 + 0.135 + 17.898$$
$$= 18.66 \text{ 1/sec} .$$

The damping constants obtained by both models are very close, and the simplified model gives a little higher value. The dominant term is due

to the dissipation in the outer irrotational flow, as should be expected.

2) For a water drop of radius 0.1 cm in air,

(a) By Marston's theory,

$$s = 4.87 \ 1/sec \ .$$

(b) By Lamb's formula

$$s = 4.49 \ Hz$$

(c) By this simplified model,

$$\omega/2\pi = 120.81 \ Hz \ (a \ given \ value)$$

$$S = S_b + S_i + S_o$$

$$= 0.378 + 4.480 + 0.241$$

$$= 5.10 \ Hz \ .$$

Again, the calculated damping constant obtained by this simplified model is close to and a little higher than the calculated value by Marston's theory. The dominant term is due to the dissipation in the inner irrotational flow, as one expects.

3) Trinh, Zwern, and Wang (1982) did some experimental work on the free oscillation of a drop in another liquid. One set of their data for phenetole drops in a mixture of water and methanol was compared with the theoretical predictions given by Marston's theory and the simplified model (Hsu 1983). This set of data was chosen because that the boundary layer was thin compared with the radius (about 10%). The damping constant predicted using the Marston's theory was about 10% lower, and

the value predicted using this simplified model was about 10% higher, than the data.

5. PHASE-FREQUENCY RELATION IN FORCED OSCILLATION

As mentioned before, the phase-frequency relation for forced oscillation is readily obtained if we know each component (both magnitude and phase) of the impedance corresponding to stiffness, inertia, and damping, respectively. Here, the impedance is defined as:

$$\text{impedance} \equiv \frac{\rho}{\Delta} \equiv \frac{\text{driving pressure (associated with quadrupole mode)}}{\text{displacement (of quadrupole mode)}}. \quad (29)$$

Thus, the phase of the displacement is relative to the driving pressure.

We compute each component of the impedance separately by the following approach. First, the phase angle is determined by physical reasoning. We then compute, by energy balance or force balance, the driving pressure associated with the quadrupole displacement described by $r = R + \varepsilon Y_2(\theta)\sin(\omega t)$.

5.1 Impedance Due to Stiffness K

The displacement of a component of pure stiffness subject to a driving force is in phase with this driving force, that is, $\xi = 0$. In the problem of an oscillating drop, stiffness is due to the interfacial tension. We may derive this component of the impedance K by employing force balance or energy balance as follows:

- 16 -

1) The fluid pressure is discontinuous at a curved surface of separation; the pressure differential is

$$p_i - p_o = \sigma(R_1^{-1} + R_2^{-1}) . \tag{30}$$

This is Laplace's formula, where R_1 and R_2 are the principal radii. Since we are only interested in the pressure variation accompanying the quadrupole oscillation, let us set $p_o = 0$ at equilibrium (the ambient pressure). Then, $p_i = \sigma(2/R)$ at equilibrium. The inner pressure p_i will not vary with the shape oscillation, since there is no volume change and there is no mass involved in this discussion. The interface is described as (see Eq. (4))

$$r = R + \varepsilon Y_2(\theta)\sin(\omega t) ,$$

which gives (Lamb)

$$1/R_1 + 1/R_2 = 2/R + (4/R^2)\varepsilon Y_2(\theta)\sin(\omega t) . \tag{31}$$

Therefore, the variation of p_o accompanying the shape oscillation due to the interfacial tension is, from Eqs. (30) and (31),

$$p_o = - (4/R^2)\sigma\varepsilon Y_2(\theta)\sin(\omega t) , \tag{32}$$

where the minus sign indicates that the outer pressure at the two poles reaches a maximum when the drop is in an oblate shape with maximum displacement. For this reason, we define the displacement Δ in the following way, so that the displacement is in phase with the driving pressure for a pure stiffness,

$$\Delta = R-r = - \varepsilon Y_2(\theta)\sin(\omega t) . \tag{33}$$

Since p_i is constant, p_o equals the driving pressure p. Thus the component of the impedance due to stiffness is

$$K = \frac{p}{\Delta} = \frac{4\sigma}{R^2} . \tag{34}$$

- 17 -

2) The potential energy, set zero when the drop is in a spherical shape at equilibrium, equals the product of the interfacial tension and the change of the interfacial area. For a small quadrupole displacement with an amplitude ε, as in Eq. (4) with $t=\pi/(2\omega)$, the potential energy is $(32\pi/5)\sigma\varepsilon^2$ (Rayleigh). The driving pressure on the interface responsible for the quadrupole displacement can be assumed to be $p = -PY_2(\theta)\sin(\omega t)$, where P is the amplitude, and the minus sign is assigned to give the correct phase angle as discussed previously (see Eq. (32)). The instantaneous power input per unit area is therefore

$$p\,\frac{d\Delta}{dt} = PY_2^2(\theta)\varepsilon\omega\sin(\omega t)\cos(\omega t) \ . \tag{35}$$

The integration of the above expression over the interface $r=R$, and over the period from $t=0$ to $t=\pi/(2\omega)$ is found to be $(8\pi/5)P\varepsilon R^2$, which should equal the potential energy, $(32\pi/5)\sigma\varepsilon^2$, corresponding to the displacement $\Delta = -\varepsilon Y_2(\theta)$ at $t=\pi/(2\omega)$. Hence $P = 4\sigma\varepsilon/R^2$. We therefore have the identical K as in Eq. (34).

5.2   Impedance Due to Inertia M

The acceleration of a mass is in phase with its driving force, so the displacement lags by 180^0 the driving force; $\xi = 180^0$. Here we compute the pressure on the interface required to drive a spherical liquid mass into the oscillation described as $r = R + \varepsilon Y_2(\theta)\sin(\omega t)$. The calculation is first carried via force balance and then via energy balance.

1) With the inviscid assumption, the velocity potential is determined by the boundary condition, as given in Eqs. (6) and (7). Then the pressure variation at both sides of the interface accompanying this potential flow is

$$p_i - P_i \left. \frac{\partial \phi_i}{\partial t} \right|_{r=R} = (1/2)\rho_i R\omega^2 \varepsilon Y_2(\theta)\sin(\omega t) \ ,$$

$$p_o - P_o \left. \frac{\partial \phi_o}{\partial t} \right|_{r=R} = -(1/3)\rho_o R\omega^2 \varepsilon Y_2(\theta)\sin(\omega t) \ .$$

The required driving pressure is $p = p_i - p_o$, and

$$p = p_i - p_o = (1/6)R\omega^2(3\rho_i + 2\rho_o)\varepsilon Y_2(\theta)\sin(\omega t) \ . \tag{36}$$

Thus the component of the impedance due to inertia, denoted by M, is, from Eqs. (29), (33), and (36),

$$M = \frac{p}{\Delta} = j^2(1/6)\omega^2 R(3\rho_i + 2\rho_o) \ , \tag{37}$$

where j is $(-1)^{\frac{1}{2}}$.

2) The kinetic energy reaches its maximum value $(4\pi/15)\omega^2 R^3(3\rho_i + 2\rho_o)\varepsilon^2$ (see Eq. (26)), when t = 0, and it is zero when $t = \pi/(2\omega)$. The driving pressure may be written as: $p = PY_2(\theta)\sin(\omega t)$, so that the acceleration, $d^2\Delta/dt^2 = \varepsilon\omega^2 Y_2(\theta)\sin(\omega t)$, is in phase with the driving pressure. For instance, when $t = \pi/(2\omega)$, the driving pressure is positive and maximum at the two poles, while the acceleration at the two poles are inward and maximum. Then, during this period, from t = 0 to $t = \pi/(2\omega)$, the power "input" is $-(8\pi/5)P\varepsilon R^2$.

This power input should equal the maximum kinetic energy, thus we obtain an expression for P and hence M.

It is worth noticing that K + M = 0 when the driving force has a frequency ω that

$$\omega^2 = \frac{24\sigma}{R^3(3\rho_i + 2\rho_o)} \, , \tag{38}$$

which is the quadrupole resonance frequency for the inviscid situation, as in Eq. (2).

5.3   Impedance Due to Viscosity

The question of what is the impedance due to viscosity is equivalent to the question of what is the driving pressure on the interface needed to supply the energy dissipation in the motion $r = R + \varepsilon Y_2(\theta)\sin(\omega t)$.

1) Let us first look at the irrotational flow. In the irrotational flow associated with the oscillatory drop, the velocity at every point is oscillating in phase, since the fluids behave incompressibly. The viscous stress, which is proportional to the spatial gradient of velocity distribution, is therefore in phase with the potential velocity. Hence, the driving pressure on the interface is in phase with the potential velocity and has a phase lead of 90° over the displacement Δ. The driving pressure, which is in phase with the velocity, is assumed in the form

$$p = -PY_2(\theta)\cos(\omega t) \, .$$

Then the instantaneous power input by the driving pressure acting on the interface is

$$\iint p\frac{d\Delta}{dt}dA = (16\pi/5)\varepsilon\omega R^2 P\cos^2(\omega t) , \tag{39}$$

which should equal the rate of energy dissipation. (a) In the inner irrotational flow, the rate of dissipation has been obtained (see Eq. (19)) as:

$$16\pi\mu_i\varepsilon^2 R\omega^2\cos^2(\omega t) .$$

By equating this rate of dissipation with the power input (Eq. (39)), we get an expression for P, $P = 5\mu_i\varepsilon/R$, which leads to B_{pi}, the component of impedance due to viscous dissipation in the inner irrotational flow,

$$B_{pi} = \frac{P}{\Delta} = j\frac{5\mu_i\omega}{R} . \tag{40}$$

(b) In the outer irrotational flow, the instantaneous rate of dissipation is (see Eq. (20))

$$(128/3)\pi\mu_o\varepsilon^2 R\omega^2\cos^2(\omega t) .$$

By equating the power input (Eq. (39)) and this rate of dissipation, we have B_{po}, the component of the impedance due to the viscous dissipation in the outer irrotational flow,

$$B_{po} = j(40/3R)\mu_o\omega . \tag{41}$$

2) Now we consider the energy dissipation only in the boundary layer, and compute the associated impedance. The velocity distribution in the boundary layer may be described as (Batchelor):

$$v(y,t) = Ue^{i\omega t}(1-\exp[-(1+j)y/\delta]) ,$$

where $Ue^{i\omega t}$ is the external stream velocity, y is the coordinate normal and relative to the boundary. The frictional stress at the boundary is the real part of the following expression (Batchelor):

$$\mu \frac{\partial u}{\partial y}\Big|_{y=0} = \mu(1+j)\frac{U}{\delta} e^{i\omega t} \ ,$$

so this skin friction has a phase lead of $\pi/4$ over the external stream velocity $Ue^{i\omega t}$. In this problem of an oscillating drop, the external stream velocity is in phase with the potential velocity, as discussed in section 3.2.1. The tangential component of the acoustic radiation stress, which is the driving force, though small, has to be in phase with the skin friction, in considering the balance of tangential stress on the interface. Therefore the phase of the radiation stress is $\pi/4$ ahead of the potential velocity and is $3\pi/4$ ahead of the interfacial displacement ; that is, $\xi=135^0$. Writing

$$p = -PY_2(\theta)\cos(\omega t + \pi/4) \ ,$$

the power input averaged over one cycle along the whole interface is then

$$(\omega/2\pi) \int_{t=0}^{2\pi/\omega} dt \iint p\frac{d\Delta}{dt} \ dA = (4\pi 2^{\frac{1}{2}}/5)\varepsilon R^2 \omega P \ , \tag{42}$$

where the contribution of the power input due to the tangential radiation stress has been neglected.

In considering the rate of dissipation, we assume the tangential radiation stress is much smaller than the normal component, so that the model of the flow distribution developed earlier is still a good

approximation for the flow in the forced oscillation. We then have the time averaged rate of dissipation in the boundary layer as given in Eqs. (22) and (23). By equating this time averaged rate of dissipation with the above time averaged power input in Eq. (42), we have an expression for P and thus obtain the component of impedance (see Eq. (29)) due to viscous dissipation in boundary layer, B_b, as:

$$B_b = [(j-1)/\sqrt{2}](2/3)\omega^{3/2}[2.25(1-c)^2(\mu_i\rho_i)^{\frac{1}{2}} + (1+1.5c)^2(\mu_o\rho_o)^{\frac{1}{2}}]. \quad (43)$$

5.4   Total Impedance

The total impedance is the vector sum of these components given in Eqs. (34), (37), (40), (41), and (43).

$$\text{impedance} = K + M + B_p + B_b, \quad (44)$$

$$\text{where } B_p = B_{pi} + B_{po} ,$$

$$= j(\omega/R)[5\mu_i + (40/3)\mu_o] ,$$

$$K = 4\sigma/R^2 ,$$

$$M = (j^2/6)\omega^2 R(3\rho_i + 2\rho_o) ,$$

$$B_b = [(j-1)/\sqrt{2}](2/3)\omega^{3/2}[2.25(1-c)^2(\mu_i\rho_i)^{\frac{1}{2}} + (1 +1.5c)^2(\mu_o\rho_o)^{\frac{1}{2}}] .$$

A schematic vector diagram of the four components is shown in Fig. 3. We obtain, finally, the phase-frequency relation as the following

$$\tan\xi = (B_p + B_b/\sqrt{2})/(K-M-B_b/\sqrt{2}) . \quad (45)$$

5.5 Comparison with the Theory by Marston

We may change the form of the phase-frequency relation derived by
Marston to get the "equivalent components of the impedance" as follows:

$$K' = 4\sigma/R^2 \ ,$$

$$M' = j^2(1/6)\omega^2 R(3\rho_i + 2\rho_o) \ , \tag{46}$$

$$B_p' = \frac{j5\omega[\mu_i^2\rho_i + (8/3)\mu_o^2\rho_o + (1/6)\mu_i\mu_o(4\rho_i - \rho_o)]}{R[(\mu_i\rho_i)^{\frac{1}{2}} + (\mu_o\rho_o)^{\frac{1}{2}}]^2} \ ,$$

$$B_b' = \frac{(j-1)25\omega^{3/2}(\mu_i\mu_o\rho_i\rho_o)^{\frac{1}{2}}}{2^{\frac{1}{2}}6[(\mu_i\rho_i)^{\frac{1}{2}} + (\mu_o\rho_o)^{\frac{1}{2}}]} \ .$$

Compared with the impedance obtained in the simplified model, they have
components of similar dependence upon parameters like density,
viscosity, and frequency at the same phase angles. The components due
to stiffness and inertia are identical. For both inner and outer
liquids of small viscosity, the value of B_b is close to the value of
B_b', whereas the value of B_p is greater than that of B_p'. Two examples
in the following show the typical numerical values of impedance due to
damping: a) For a hexane drop in water, $\rho_i = 0.655$ g/cm^3, $\mu_i = 0.29$ cp,
$\rho_o = 0.997$ g/cm^3, $\mu_o = 0.89$ cp. We have $B_b = 0.15\omega^{3/2}$, $B_b' = 0.13\omega^{3/2}$, whereas
$B_p = 0.13\omega/R$, $B_p' = 0.07\omega/R$.

b) For a p-xylene drop in water, $\rho_i = 0.857$ g/cm^3, $\mu_i = 0.614$ cp.

Therefore, $B_b = 0.22\omega^{3/2}$, $B_b' = 0.17\omega^{3/2}$; $B_p = 0.15\omega/R$, and $B_p' = 0.05\omega/R$.

Fig. 4 illustrates the phase-frequency relation for a hexane drop in
water predicted by Marston's theory and the simplified model

respectively with given drop size and properties of the liquids
(interfacial tension, density, and viscosity). This figure is meant to
be representative, and good agreememt between the simplified model and
Marston's theory is shown. This simplified model has some potential
advantages. For example, it may be difficult to apply the direct
approach to drops in special geometries, e.g., non-spherical. But
approximate flow distributions may still be obtainable by combining
irrotational flow with boundary layer along the interface. For an
interface having viscous or elastic properties, the model may be
modified by incorporating the extra impedance components into it; one
example will be shown later in this article.

6.   SOME APPLICATIONS

One of the applications of the oscillations of drops is the measurement
of the interfacial tension between the drops and the surrounding
liquids. Based on the theories, the interfacial tension can be inferred
from the phase-frequency measurement given the size of the drop and
density as well as viscosity of the both liquids. We did measurements
for the interfacial tensions between various liquids, such as
water-hexane, water-propane(superheated), and water-hexane-surfactant.
One experimental technique called acoustic levitation was adapted and
showed essential importance (Apfel 1976). The block diagram of our
experiment apparatus is shown in Fig. 5. A strong acoustic standing
wave can be established in a host liquid, water in this work, and can
produce an acoustic radiation force on an immersed drop. The acoustic

- 25 -

force can be adjusted to counterbalance the gravitational force; then the drop is acoustically levitated. Superimposed on this levitation acoustic force, via the same transducer, we can introduce another modulated acoustic force to drive the drop into oscillations. The oscillation is enhanced when the modulation frequency is near the (quadrupole) resonance frequency of the drop. The oscillations of the drop is detected by an optical method adapted from one work of Trinh, Zwern, and Wang (1982). Details about the apparatus and procedures are described elsewhere (Hsu 1983) (Hsu & Apfel 1984).

There are several special advantages of this technique for measuring interfacial tension. The interface between the two fluids is free from contact with any solid object. The host liquid can be a very clean and smooth container for the drop. Therefore, measurements can be conducted even with the liquid of the drop in a metastable state, such as the superheated state. Also, the drop can be held in the host very steadily in a certain position for hours. It allows accurate measurements of the drop's size, oscillation frequency, and phase with comparative ease. Sometimes the interfacial tension may change over time due to contamination or changes in environmental conditions. With the tracking feature built into our apparatus, we can automatically monitor the change of the interfacial tension with time (Hsu & Apfel 1984).

6.1 Data Reduction

6.1.1 Approximation by Newton's Iteration

The phase-frequency relation for quadrupole oscillations of drops may be
expressed by the following equation, according to the model derived by
Marston,

$$T = (\alpha\omega^{3/2} + \gamma\omega)/(\omega^{*2} - \alpha\omega^{3/2} - \omega^2) , \qquad (47)$$

where ω^* is the inviscid resonance frequency and is related directly to
the interfacial tension to be measured as in Eq. (2), $T = \tan\xi$, ξ is the
phase angle of the drop's displacement with respect to its driving
force, ω is the frequency of the forced oscillation, α and γ are
functions of the drop's size and of the properties (density and
viscosity) of the host as well as the drop liquid (Marston 1980). The
phase-frequency relation given by the simplified model derived in this
manuscript can also be expressed in the same form as Eq. (47), though α
and γ will then represent different functions of the size and the
properties; α corresponds to B_b, and γ corresponds to B_p (see Fig. 3).

In the work done by Marston and Apfel (1980) Eq. (47) was
approximated in the following way and then employed with data for
deducing interfacial tension. First, Eq (47) may be rewritten as a
function of ω,

$$f(\omega) = T\omega^2 + \alpha(1+T)\omega^{3/2} + \gamma\omega - T\omega^{*2} = 0 . \qquad (48)$$

By applying Newton's method of iteration, and using ω^* as an initial
approximation, ω can be expressed as a function of T (Uspensky) (Marston
1980),

- 27 -

$$\omega \simeq \omega^* - \frac{f(\omega^*)}{f'(\omega^*)} \tag{49}$$

$$\simeq (\omega^* - \tfrac{1}{2}\alpha\omega^{*\frac{1}{2}} + 3/8\alpha^2) - 1/T \; (\tfrac{1}{2}\alpha\omega^{*\frac{1}{2}} - 3/4\alpha^2 + \tfrac{1}{2}\gamma) \; .$$

Therefore,

$$\omega(90^0) \simeq \omega^* - \tfrac{1}{2}\alpha\omega^{*\frac{1}{2}} + (3/8)\alpha^2 \; , \tag{50}$$

and

$$\omega(\xi) \simeq \omega(90^0) - 1/T[\tfrac{1}{2}\alpha\omega^{*\frac{1}{2}} - (3/4)\alpha^2 + \tfrac{1}{2}\gamma] \; . \tag{51}$$

Notice that the resonance frequency $\omega(90^0)$ is a function of ω^* (which is a function of the stiffness and mass) and α, but not of γ. This once again demonstrates the fact that the impedance of 90^0 phase plays no role in determining the resonance frequency $\omega(90^0)$. The damping constant s may be defined as

$$s = [\omega(\xi) - \omega(90^0)] \cdot (-T) \; . \tag{52}$$

It can be determined experimentally. On the other hand, from Eq. (51), we have

$$s \simeq \tfrac{1}{2}\alpha\omega^{*\frac{1}{2}} - (3/4)\alpha^2 + \tfrac{1}{2}\gamma \; . \tag{53}$$

We can therefore predict the value of the damping constant with known densities, viscosities, and the interfacial tension of the two liquids. In our measurements for hexane and pentane drops in water, there is good agreement (difference within 20%) between the measured and the predicted damping constant. Substituting s into Eq. (50), we have

$$\omega^* \simeq \omega(90^0) + \tfrac{1}{2}\alpha\omega^{*\frac{1}{2}} - (3/8)\alpha^2 \; ,$$
$$= \omega(90^0) + s + (3/8)\alpha^2 - \tfrac{1}{2}\gamma \; . \tag{54}$$

Furthermore, by neglecting the last two terms of Eq. (54), we have

$$\omega^* \simeq \omega(90^0) + s \; . \tag{55}$$

Eq. (55) was used to infer interfacial tensions from measurements in the work done by Marston and Apfel (1980) and also in this work. In this way, α and γ were not involved in the calculation for interfacial tension.

A bias is introduced by neglecting the last two terms of Eq. (54). It can be estimated by calculating the α and γ according to theories. For the interface between water and hexane, Eq. (55) gives ω^* too high by 0.8% according to Marston's theory, or too high by 1.5% according to the simplified model. Therefore the difference between Marston's theory and the simplified model in inferring interfacial tension from data is 0.7% in ω^* or 1.5% in interfacial tension for the water-hexane interface.

6.1.2   Extra Impedance due to Interfacial Viscosity

The above approximation can be applied well to the measurements such as hexane or pentane drops in water. However, we observed that the measured values of s could increase by a factor of 2 or more when the interface is contaminated. Considering the parameters in Eq. (53), the change of the condition in the interface should change α , which can be traced to the damping in the boundary layer, but should not change γ, which can be traced to the damping in the potential flow. In Eq. (43), parameter c should vary as the condition in the interface changes. For example, we may arbitrarily set c=0; it implies that the interface can

move only in the radial direction but not in the tangential direction. Nevertheless, for two liquids with similar viscosity, such as water and hexane, the corresponding change in B_b is small, and the corresponding change in s (according to Eq. (53)) is far less than the observed factor of 2. Therefore, we judge that in these cases some significant contribution to the damping resides in the interfacial viscosity (Miller & Scriven 1968). We can derive the component of impedance attributed to this interfacial viscosity in a manner similar to the derivation for other components (see Appendix). The phase angle of this component is 90^0, and the magnitude is $2\kappa\omega/R^2$, where κ is the coefficient of interfacial dilatational viscosity. By the argument mentioned before, the resonance frequency $\omega(90^0)$ does not depend on this component. But the damping constant should be modified to be

$$s = \tfrac{1}{2}\alpha\omega^{*\frac{1}{2}} - (3/4)\alpha^2 + \tfrac{1}{2}\gamma + 12\kappa/(R^3\Gamma). \qquad (56)$$

The data reduction procedure is thus modified as follows for the situations where the interfacial viscosity is significant. When Eq. (55) is applied for inferring interfacial tension, the quantity s should be the theoretical value assuming no interfacial viscosity (Eq. (53)). The coefficient of the interfacial viscosity κ can then be inferred from the difference between the measured damping constant (Eq. (52)) and the theoretical prediction assuming $\kappa=0$.

6.2   Some Examples

We have applied this experiment technique to several kinds of

interfaces. The host liquid was water in all cases. The size of the

drops ranged between 1 to 2 mm in diameter. The amplitude of the

oscillations was in the order of 1% of the radius. All measurements

were conducted at room temperature and at atmospheric pressure. The

details of these experiments is described elsewhere (Hsu 1983) (Hsu &

Apfel 1984). Here, we briefly summarize the results.

1) water-hexane and water pentane: For the water-hexane interface,

the inferred interfacial tension (using Eq. (55) without the correction

for its bias) is 51.4 dyne/cm while the literature data is 51.1 dyne/cm.

For water-pentane interface, the inferred value is 49.5 dyne/cm while

the literature data is 49.0 dyne/cm. The uncertainty of our interfacial

tension measurement owing to the uncertainty in size, frequency, and

density is estimated at 0.65%. The measured values of the damping

constant agree well with theoretical prediction. The ratio of $s/\omega(90^0)$

is about 4.5% for hexane drops in water and 3.7% for pentane drops in

water.

It seems logical that we should be able to deduce information on

the viscosity of either the drop or the host from the measured damping

constant. However, it appears that the damping constant is not

sensitive enough to the change of viscosity of one liquid (Hsu 1983);

thus, with the precision of our experiment, it is not practical to get

any significant information about the viscosity of either the inner or the outer fluid from the measurements.

2) water-propane, water-isobutane, and water-butane: At one atmosphere pressure, the boiling points of propane, isobutane, and butane are $-42.1^\circ C$, $-11.7^\circ C$, and $-0.5^\circ C$, respectively. Therefore, the samples were superheated by about $64^\circ C$ to $23^\circ C$ in our measurements. The inferred interfacial tension is 52 dyne/cm for water-propane, 50 dyne/cm for water-isobutane, and 48 dyne/cm for water-butane. In the water-propane measurements, the drops dissolved in water gradually, and the interfacial tension decreased gradually with time presumably due to the increase of the concentration of propane in water near the interface. The superheated drops were first formed in one kind of gel under pressure, then the pressure was released and the drops were transported together with the gel into the host water (Apfel). Though the gel used was water soluable and was determined to be non-surface-active, the measured damping constant did show significant interfacial viscosity probably due to trace amount of residue of the gel in the interface. This raised the uncertainty of these measured interfacial tensions. The same procedure was applied to some hexane and pentane drops. The inferred interfacial tension is lower than that for non-contaminated interface: 47.3 dyne/cm for water-hexane, and 45.5 dyne/cm for water-pentane; the damping constant is greater by a factor of 2 to 3. The coefficient of interfacial dilatational viscosity κ calculated from these data is in the order of 0.01 dyne sec/cm. Thus

the interfacial viscous stress is in the order of 0.1 dyne/cm for the amplitude of oscillations in our measurements. For the water-hexane interface and the κ of this magnitude, in Eq. (56), the magnitude of the last term (about 6% of $\omega(90^0)$) is greater than the sum of the rest terms (about 4.5% of $\omega(90^0)$).

3) water-hexane-surfactant: Measurements have been made for the interfacial tension between water and hexane with some surface active agents dissolved in one of the two phases. For example, different concentrations of sodium dodecyl sulfate dissolved in water or of tetradecanol dissolved in hexane have been used. When the drop to be measured was introduced into the host liquid, the surfactant molecules packed into the interface, and the interfacial tension decreased until this system reached equilibrium. With the automatic tracking feature built into our apparatus, we got the history of the interfacial tension after the drop was introduced. The final equilibrium interfacial tension in our measurements showed good agreement with literature data taken with static methods (Hsu & Apfel 1984). The measured damping constants were about 50% higher than the theoretical prediction assuming there is no contamination. The interfacial viscosity thus can be estimated as in the order of 0.002 dyne·sec/cm.

7. SUMMARY AND CONCLUSIONS

A simplified model has been developed for describing the motion of a drop oscillating in its quadrupole mode in a host liquid. In this model the potential (bulk) flow in the outer (host) and inner (drop) fluids as well as the boundary layer in the outer and inner fluids contiguous to the interface were superimposed in an ad hoc manner to describe the whole flow. The viscous dissipation in both the bulk flow and the boundary layer was calculated; so was the total energy of the motion. From these calculations, the rate of damping of the oscillations was obtained. For the case of forced oscillation, the components of impedance owing to the stiffness (interfacial tension), the mass, the viscous dissipation in the bulk flow, and the viscous dissipation in the boundary layer were evaluated individually. The vector sum of these impedance components gave the phase between the drop's response and the driving force at different frequencies.

The damping rate and the phase-frequency relation deduced from this simplified model agree well with that given by previous theories (e.g. Marston's) which were derived in an exact approach. This model may have special advantages in some situations; for example, if the equilibrium shape of the drop is non-spherical or if the interface exhibits some elastic or viscous characteristics different from the two fluids. For the interface having a dilatational interfacial viscosity, the extra impedance and damping attributed to it were derived. Though the derivation of this simplified model was specific to the quadrupole mode, the procedure should be applicable to oscillations of higher modes.

- 34 -

As an application, the interfacial tension between the drop and the host can be experimentally determined based on the phase-frequency relation. An experiment technique by acoustic means was briefly introduced. Some results for different interfaces such as water-hexane, water-propane (superheated by 65 Celsius degrees), and water-hexane-surfactant were reported.

APPENDIX

We assume that the interfacial viscous forces depend on the interfacial rate of strain and can be expressed as

$$\kappa[d(\delta A)/dt]/\delta A \ ,$$

where κ is the coefficient of interfacial dilatational viscosity, and δA is the differential interfacial area, and

$$\delta A = 2\pi r \ \sin\theta \ r \ d\theta \ .$$

We may consider the interfacial strain in two orthogonal directions.

1) In the direction of θ: The rate of deformation is

$$d(rd\theta)/dt = (dr/dt) \ d\theta \ .$$

The rate of strain is therefore

$$(dr/dt)/r$$

The corresponding stress per unit length is

$$\kappa(dr/dt)/r$$

The power dissipation owing to this interfacial viscosity is ($\theta=0$ to π)

$$\int \kappa(dr/dt/r) \cdot 2\pi r \sin\theta \cdot (dr/dt)d\theta$$

$$=(16\pi/5)\kappa\varepsilon^2\omega^2\cos^2(\omega t)$$

- 35 -

with the displacement defined as in Eq. (33).

2) In the direction of ϕ: We have the rate of deformation

$$2\pi\sin\theta(dr/dt)$$

and the rate of strain is

$$(dr/dt)/r \ .$$

The corresponding power dissipation is ($\theta=0$ to π)

$$\int \kappa(dr/dt/r)\cdot(rd\theta)\cdot2\pi\sin\theta(dr/dt)$$

$$=(16\pi/5)\kappa\varepsilon^2\omega^2\cos^2(\omega t) \ .$$

The phase of this component is considered by the following argument:
The driving force should be in phase with the viscous stress. The
viscous stress is in phase with the rate of strain which leads the
displacement by 90^0. Therefore, the phase of the impedance component
due to the interfacial viscosity is 90^0. Then we can calculate the
instantaneous power input with an assumed amplitude of the driving force
(see Eq. (39)) and equate this power input to the above power
dissipation. The magnitude of the impedance is thus obtained as
$j2\kappa\omega/(r^2)$.

REFERENCES

Apfel, R.E., 1976, J. Acoust. Soc. Am., 59(2), pp. 339-343.

Apfel, R.E., U.S. pat. 4, 143, 274.

Batchelor, G.K., 1967, An Introduction to Fluid Dynamics, Cambridge University Press, London.

Hsu, C.J., Ph.D. thesis, Yale University, Dec. 1983.

Hsu, C.J. & Apfel R.E., 1984, submitted to J. Colloid Interface Sci..

Lamb, H., 1945, Hydrodynamics, sect. 275, 355, Dover, New York.

Lock, R.C., 1951, Quart. Journ. Mech. and Applied Math., Vol. IV, Pt. 1.

Marston, P.L., 1980, J. Acoust. Soc. Am., 67(1), pp. 15-26.

Marston, P.L. & Apfel R.E., 1980, J. Acoust. Soc. Am., 67(1), pp. 27-37.

Miller, C.A. & Scriven, L.E., 1968, J. Fluid Mech., vol. 32, part 3, pp. 417-435.

Rayleigh, J.W.S., 1945, Theory of Sound, sect. 364, Dover, New York.

Trinh, E., Zwern, A., & Wang, T.G., 1982, J. Fluid Mech., vol. 115, pp. 453-474.

Uspensky, J.V., 1948, Theory of Equations, McGraw-Hill, New York, pp. 174-177.

$j\omega b$

$j^2\omega^2 m$ K
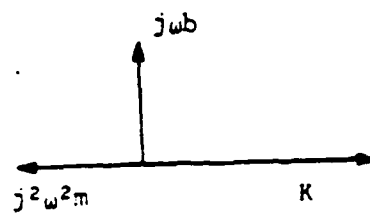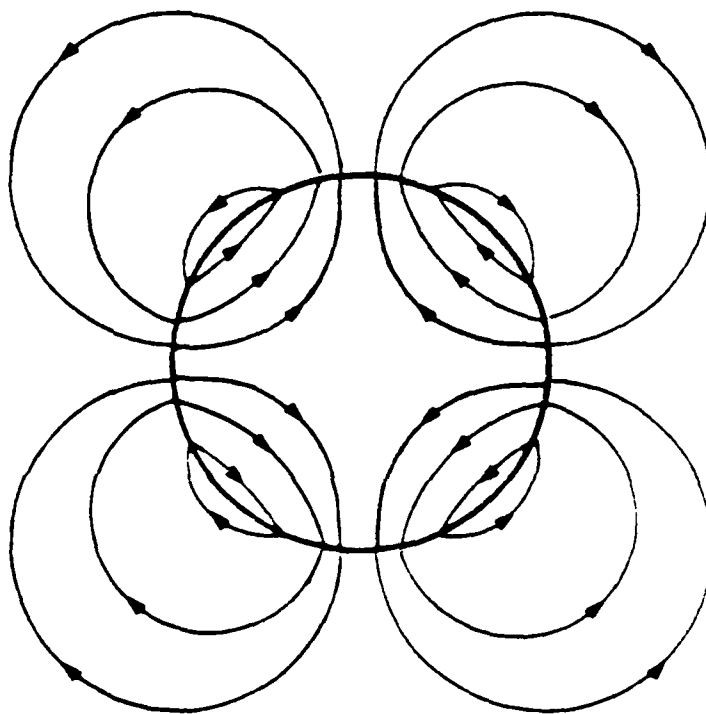
figure 1.

Figure 2 : Schematic stream line pattern resulting from quadrupole
oscillation of a drop in an host; inviscid flow was assumed.
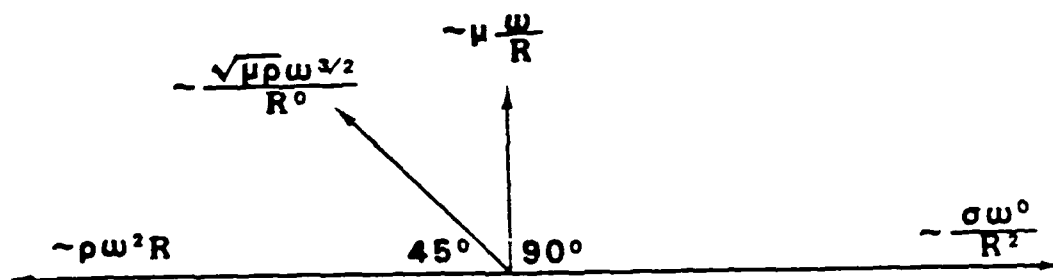
Figure 3. Schematic impedance diagram for the quadrupole oscillation of a drop-host system.
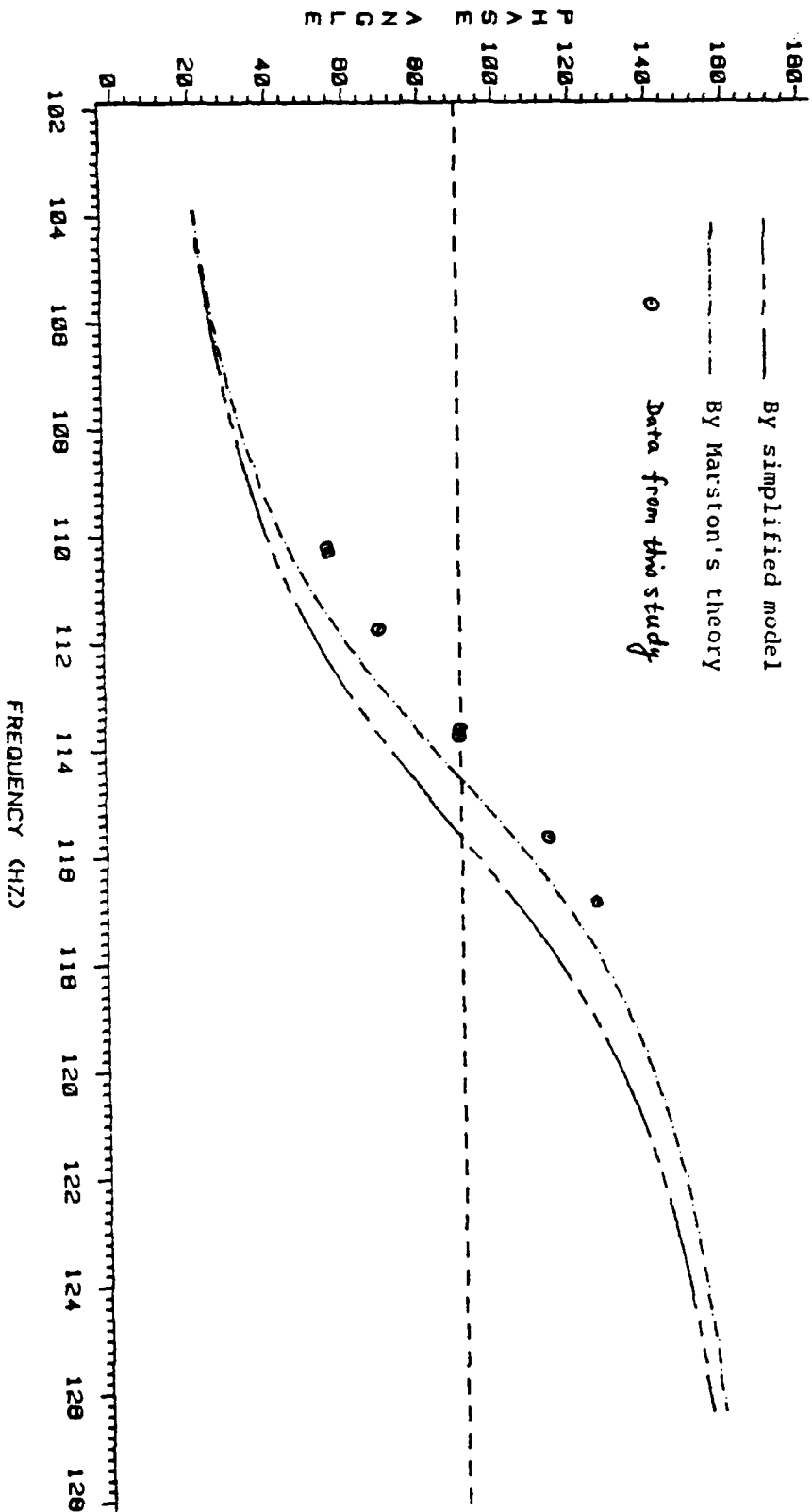
Figure 4. Phase vs. frequency curves given by the simplified model and Marston's theory respectively: Example for host, water; drop, hexane; drop radius, 0.0825 cm.
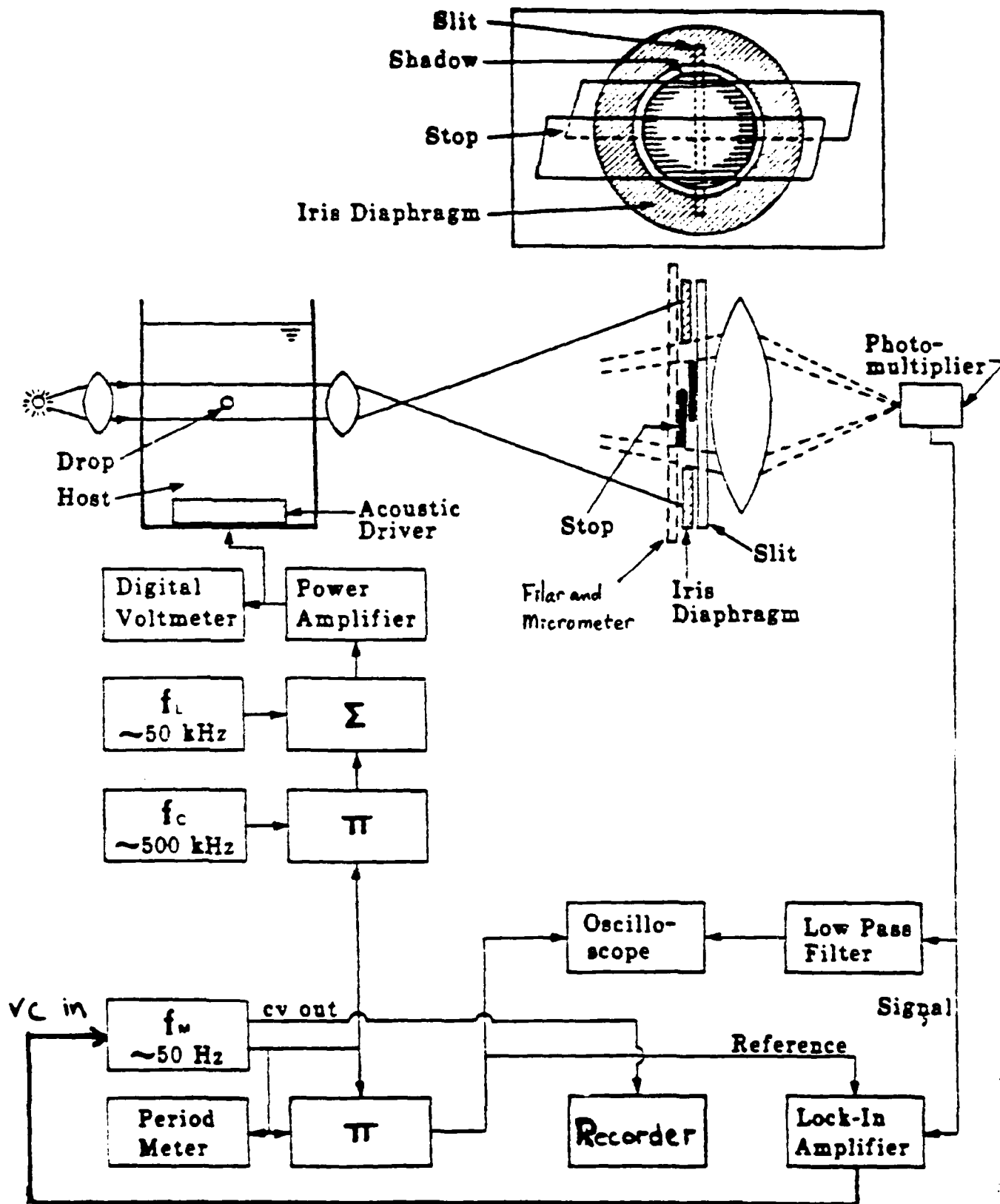
Legend:
—— By simplified model
—·— By Marston's theory
⊖ Data from this study

PHASE (DEGREE)

FREQUENCY (HZ)

Figure 5. Diagram of apparatus.

A TECHNIQUE FOR MEASURING INTERFACIAL TENSION BY
QUADRUPOLE OSCILLATIONS OF DROPS

Chaur-Jian Hsu and Robert. E. Apfel

Yale University

1984

A technique for measuring interfacial tension is presented. A drop of one liquid is acoustically levitated in another liquid (host) and is also acoustically driven into quadrupole shape oscillations. The interfacial tension is inferred from the resonance properties of the drop, provided that the size of the drop and the densities of the two liquids are known. The relevant results of theories are mentioned. The apparatus and procedure are described. Some special features of this technique are discussed; for example, the drop has an indefinite life time, the interface has no contact with any solid surface, and any changes of the interfacial tension can be tracked automatically. Data for the interfaces such as water-hexane, water-propane (superheated by 65 Celsius degrees), and water-hexane-surfactant are reported.

1. INTRODUCTION

Interfacial tension is a subject of importance for practical applications as well as in basic research. There are many methods available for measuring interfacial tension. In this article, we present one technique which has unique advantages in some special situations. One example is that one of the two liquid phases is in metastable state, i.e., superheated or supercooled. Another example is that the interfacial tension changes with time due to some changes in the environment, such as pressure, temperature, or addition of surface active material into the interface. In the first example, any contact between the metastable liquid and a solid surface will easily trigger the onset of nucleation; this contact imposes difficulty on applying any traditional methods. In the second example, the pendant-drop method is probably the best method available previously (1) for measuring the interfacial tension as a function of time. However, the pendant-drop method requires taking linear measurement of a nonspherical surface (1) repeatedly, and it is questionable that whether a significant decrease of interfacial tension can be measured with this method.

The basic idea of the technique described in this article is similar to that of the traditional dynamic methods such as the oscillating drops method. The interface is disturbed so that it displaces away from the equilibruim position; the restoring force is measured, and the interfacial tension can be inferred if it provides the

- 2 -

restoring force. On the other hand, there are some significant differences between this technique and the traditional oscillating drops method: 1) the drop is acoustically levitated (2) in another liquid, 2) the drop is driven into oscillation by an acoustic force, and 3) the changes of interfacial tension can be automatically tracked with a phase-lock feedback scheme built into this technique.

Because the drop can be levitated almost indefinitely, the drop's size, the resonance frequency associated with quadrupole oscillations, and other parameters can be measured very accurately with comparative ease. Because there is no solid surface in contace with the drop, the liquid of the drop can be in a metastable state and survive for long enough time for conducting a measurement. Because of the long life time of drops and the tracking feature, any changes of interfacial tension can be monitored automatically. Another advantage of this method is that it takes only a small amount of the drop liquid (~microliter). It could be important when a significant amount of the liquid is not readily available. In the rest of this article, we will first briefly introduce the theoretical background. Then the apparatus and experiment procedures will be described. Some applications and data will be reported as examples.

2. THEORETICAL BACKGROUND

Since details of the theories are described elsewhere (3) (4), we only briefly summarize the results.

It is known that the resonance frequency of a basic driven spring-mass system is

$$\omega(90^0) = (k/m)^{\frac{1}{2}} .$$

where k is the stiffness of the spring, m is the mass, and the resonance frequency is defined as the frequency at which the phase between the driving force and the displacement of the mass is 90^0. Therefore, if the $\omega(90^0)$ and m are known, the stiffness can be obtained. The above relation holds regardless of the damping as long as the damping force is in phase with the velocity (that is, 90^0 with the displacement).

There is a similar expression for the resonance frequency of a drop oscillating in quadrupole mode in another fluid (5).

$$\omega^* = \left[\frac{24\sigma}{R^3(3\rho_i + 2\rho_o)} \right]^{\frac{1}{2}} . \tag{1}$$

where ω^* is the angular frequency, σ is the interfacial tension, ρ_i and ρ_o are the densities of the inner (drop) and outer (host) liquid respectively, and R is the radius of the drop. Fig. 1. shows schematically the extreme positions of a drop oscillating in quadrupole mode, that is, in prolate and oblate shape alternatively. The above equation was derived based on the inviscid assumption, which is a good approximation when the viscosity and density of two fluids are very

- 4 -

different such as a liquid drop in gas or a gas bubble in liquid.
However, for a liquid drop in another liquid, the above inviscid
resonance frequency ω^* is not the same as the frequency of 90^0 phase
owing to the nature of the viscous damping in the boundary layer
continguous to the interface (3) (6).

Marston (3) derived the phase-frequency relation for the forced
oscillation of a drop in another liquid, assuming both liquids have
small viscosity. The resultant equation is

$$\omega^* \simeq \omega(90^0) + s , \tag{2}$$

where ω^* is the inviscid resonance frequency as in the Eq. [1], s is
called damping constant which is about 5% to 10% of the resonance
frequency $\omega(90^0)$ for the liquids we have studied. The quantity s can be
calculated as a function of the interfacial tension, density, and
viscosity of the two liquids. It can be also obtained experimentally
making use of the following relation:

$$s \simeq [\omega(90^0) - \omega(\xi)] \bullet \tan(\xi) . \tag{3}$$

where ξ denotes a certain phase angle different than 90^0. A bias is
introduced by the approximation made in the derivation of s in Eq. [2]
(4). This bias depends on the theory used to derive s. For the
interface between water and hexane, Eq. [2] gives ω^* too high by 0.8%
according to Marston's theory, or too high by 1.5% according to the
simplified model (4).

In practice, ξ is taken as several different phase angles around 90°, and the averaged s is used for obtaining ω^*. Therefore, the interfacial tension can be inferred experimentally in this way: measure $\omega(90°)$ and $\omega(\xi)$ to get s and ω^*

then #s# can be calculated with the measured R and known ρ_i and ρ_o.

Hsu and Apfel (6) (4) have recently developed a simplified model for analyzing the quadrupole oscillations of a drop in liquid, which gives results that agree well with the above results from Marston's theory. In the simplified model, an "interfacial dilatational viscosity" (7) was introduced. The interfacial dilatational viscosity κ has a dimension of force·time/length, and it relates the viscous force and the interfacial rate of strain. It has been found that the damping constant increases due to κ by this amount $12\kappa/[R^3(3\rho_i+2\rho_o)]$, which could be comparable with the damping due to viscous dissipation in the inner and outer liquids when the interface is contaminated. On the other hand, the resonance frequency $\omega(90°)$ is not dependent on κ, because the interfacial stress has a phase of 90° relative to the drop's displacement. Therefore, when the interfaces are contaminated and when Eq. [2] is applied for inferring interfacial tension, the quantity s should be the theoretical value assuming no interfacial viscosity (4). The coefficient of the interfacial viscosity κ can then be inferred from the difference between the measured damping constant (Eq. (52)) and the theoretical prediction assuming $\kappa=0$.

- 6 -

3. APPARATUS AND PROCEDURE

The block diagram for the apparatus is shown in Fig. 2. The equipment in Fig. 2 may be described in four parts. The first part is the apparatus used to levitate a drop in water and to drive the drop into shape oscillations (8). The second optically detects the drop's shape oscillations and converts the oscillations into electric signals. The third part provides a feedback loop to track the resonance frequency of the drop or the frequency of any selected phase. The fourth part takes measurement of the diameter of the drop. They are described as follows.

3.1 Levitation and Shape Oscillation

The levitation cell, which holds the host liquid and transducer, is a box with a cross section of 5.4 cm square and a height of 11 cm. The box is made of Lucite plates, 3.18 mm in thickness for the walls and 6.35 mm for the bottom, and it is open at the top. The transducer, which converts electric energy into mechanical motion and generates waves in the host water, is a Channel Industries (Santa Barbara, CA) 5400, Lead Zirconate Titanate piezoelectric ceramic disk with a diameter of 3.9 cm and a thickness of 1.3 cm. The transducer is immersed in water and sits on the bottom plate of the cell. The host liquid in the levitation cell is water for all experiments in this study.

At certain water level and frequency, the transducer-water-cell system resonates and generates standing waves in the water column. A

drop of a liquid other than water in this standing wave field is subject
to an acoustic radiation force (9), which is a time averaged (dc) second
order effect of the wave. This force tends to drive the immersed drop
toward a position of maximum pressure if the drop is more compressible
than the water "host", while gravity tends to push the drop up or to
pull it down depending on the densities of the drop and the host. If
the drop can find a position where the acoustic radiation force
counterbalances the gravitational force, it is acoustically levitated at
that position. The radial pressure distribution (maximum at the center)
forces the drop to the c_nter of the water column if the drop is more
compressible than the host.

Distilled water is fed into a Barnstead Nanopure-A 4-holder system,
and circulates through the system to reach a resistivity, which
indicates the purity, of 17.7 - 17.9 megohm/cm. The levitation cell,
the transducer, and others like syringes and needles are kept away from
dirt and are flushed a few times with the clean water before an
experiment is conducted. The clean water is degassed and then slowly
poured into the levitation cell. Then we place the transducer at the
center of the bottom of the cell. There are no bubbles visible in the
cell when an experiment is performed.

We tune the levitation system by adjusting the water level and
sweeping the levitation frequency so as to maximize the current going
through the transducer. The water level (about 8.3 cm from the top of

- 8 -

the bottom plate) and the levitation frequency (about 52 kHz) that we choose provide stable levitation for hours at low voltage (about 4 V for hexane drops). The volume of water in the cell is about 220 cm^3. The levitation position is about at the middle of the height of the water column.

To levitate a drop, we introduce it into the bottom part of the cell (using a threaded syringe) and trap it as it rises (all the liquids to be measured in this study are less dense than water) by turning on the levitation voltage. The drop's radius is in the order of 1 mm.

The equilibrium shape of the drop is determined by the interfacial tension, gravity, and the local distribution of the acoustic radiation pressure. In our experiments, the equilibrium shape of the levitated drops is nearly spherical. The difference between the diameter taken horizontally and vertically is less then 0.1% of the diameter.

At a higher resonance frequency of the transducer-water-cell system (about 510 kHz), the wavelength is comparable to the diameter of the drop, the radiation force is stronger (3), and the deformation of the drop is greater. Furthermore, we turn this acoustic radiation force on and off at a frequency matching the quadrupole resonance frequency of the drop (about 100 Hz) in order to enhance the drop's oscillation; this can be done by modulating this high frequency signal. In our experiments, the amplitude of the drop's oscillation is in the order of 1% of the drop's radius.

Therefore, three sinusoidal electric signals are combined in such a way to give v_t driving the transducer, that is

$$v_t = v_l + v_c \cdot v_m .$$

According to their functions, we call these signals the levitation signal (~52 kHz), the carrier signal (~510 kHz), and the modulation signal (~50 Hz), associated with subscripts l, c, and m, respectively. The rms voltage level is about 4 V for v_l, and about 5 V for v_t.

3.2   Detection of Shape Oscillation

An optical method adapted from an experimental work done by Trinh, Zwern, and Wang (10 is used for detecting the shape oscillations of drops. This method is non-invasive and provides adequate sensitivity.

As shown in Fig. 2, the (white) light beam passes horizontally through the levitation cell, then is enlarged by a lens and is projected and focused onto a plate with a slit on it. The slit is vertical with a width about 1 mm and a height about 5 cm. The light through the slit is focused onto the sensing surface of a photomultiplier (ENI type 9798B). The shadow of a levitated drop centers across the slit and blocks part of the light going through the slit. When the drop oscillates in its quadrupole mode, the amount of light going through the slit changes accordingly; therefore, an ac voltage signal coherent with the drop's oscillation is obtained. We use a dc power supply at 1000 V to 1200 V

- 10 -

for the photomultiplier. The stop and the iris diaphragm reduce the
light going through the slit and result in two advantages. First, the
photomultiplier can operate at a higher sensitivity to give a stronger
ac signal for a given amplitude of a drop's oscillations. Secondly, the
noise due to light scattering by particles in the path of the light beam
is reduced.

3.3 Phase-lock Loop and Frequency Measurement

The phase-lock feedback loop is formed by feeding the dc output of the
LIA (lock-in amplifier) into the v.c. (voltage control) input port of
the generator of the modulation signal. Fig. 3 shows the loop
schematically. The output of the generator represents the driving
force, and the output from the drop represents its response. To perform
the measurement, we first have the v.c. input disconnected, set the
phase dial of the LIA to zero, manually sweep the frequency of the
generator around the drop's quadrupole resonance and set the frequency
to null the dc output of the LIA, and then connect the dc output of the
LIA to the v.c. input port. If the frequency set on the dial is indeed
the resonance frequency of the drop, then the phase between the two
inputs of the LIA is 90^0, and the output of the LIA is zero. Thus the
output of the generator stays on the same frequency. If the interfacial
tension, or correspondingly the resonance frequency of the drop,
changes, the phase is no longer 90^0 and the output of the LIA is
non-zero, which then changes the frequency of the generator's output.

With adequate sensitivity and polarity of the LIA, the resonance frequency, or equivalently the interfacial tension, can be tracked automatically. The key point here is that the LIA can take two inputs with the phase between them only slightly different from 90° and provide a dc level great enough to control the frequency to be very close to the resonance frequency, which implies a phase very close to 90°.

The frequency to be measured can be read from the frequency counter , or can be converted into voltage and recorded on a X-Y recorder with a time base so as to plot the "history" of the interfacial tension of one measurement (i.e. Fig. 5). The frequencies corresponding to phase angles other than 90° can be obtained similarly by changing the phase dial on the LIA accordingly.

3.4   Phase-lock Loop for Levitation System

The above idea of phase-lock feedback is also applicable for the levitation system. A similar schematic diagram is shown in Fig. 4. Here, the generator is for the levitation signal, and the output from the levitation system is the output of the current probe hooked on one of the two leads of the transducer. Its function is to adjust automatically the levitation frequency to compensate for the change of the sound speed in the host water due to the change of temperature (about 1°C rise after 1 hour levitation). It appears helpful in stablizing the drops for experiments need to levitate the drops for a few hours.

3.5   Size Measurement

The diameter of the shadow of the levitated drop is measured near the plane of the slit. After the frequency measurement, the drop is released, and two precision rods of known diameters are placed through the levitation position and have the diameters of their shadow measured individually. This way the size of the drop can be calculated with an accuracy within 0.15%. A filar system adapted with translational stages and a micrometer is used to measure the size of the shadow. A filar telescope with magnification of 20 and a ruler horizontally affixed to the plate with the slit on it serve to mark the position of the levitated drop in three dimensions.

3.6   Density Measurement

The densities of the sample liquids are measured using a Mettler/Parr DMA-40 densitometer. The uncertainty of this measurement is less than 0.1%.

4.   SOME EXAMPLES

We have applied this experiment technique to several kinds of interfaces. The host liquid was water in all cases. The size of the drops ranged between 1 to 2 mm in diameter. The amplitude of the oscillations was in the order of 1% of the radius. All measurements were conducted at room temperature and at atmospheric pressure.

4.1 Water-hexane And Water-pentane

Fig. 5 shows one set data of a hexane drop of radius 0.0825 cm in water, along with the theoretical prediction by the Marston's theory and by the simplified model assuming literature values for interfacial tension, density, and viscosity. The data points follow the slope of the theoretical line closely, which indicates agreement between the measured and theoretical damping constant. The measured frequencies associated with 90^0 and other phase angles are less than the theoretical prediction, which indicates that the measured interfacial tension is less than the literature value. For the water-hexane interface, the inferred interfacial tension (using Eq. [2] without the correction for its bias) is 51.4 dyne/cm while the literature data is 51.1 dyne/cm. For water-pentane interface, the inferred value is 49.5 dyne/cm while the literature data is 49.0 dyne/cm. The uncertainty of our interfacial tension measurement owing to the uncertainty in size, frequency, and density is estimated at 0.65%. The measured values of the damping constant agree well with theoretical prediction. The ratio of $s/\omega(90^0)$ is about 4.5% for hexane drops in water and 3.7% for pentane drops in water. The liquid samples were from Aldrich Chemical Company, Inc.: n-hexane with 99+% purity, catalog #13938-6; n-pentane with 99+% purity, catalog #15495-4.

It seems logical that we should be able to deduce information on the viscosity of either the drop or the host from the measured damping constant. However, it appears that the damping constant is not

sensitive enough to the change of viscosity of one liquid (6); thus, with the precision of our experiment, it is not practical to get any significant information about the viscosity of either the inner or the outer fluid from the measurements.

4.2 Water-propane, Water-isobutane, And Water-butane

At one atmosphere pressure, the boiling points of propane, isobutane, and butane are -42.1^0C, -11.7^0C, and -0.5^0C, respectively. Therefore, the samples were superheated by about 64^0C to 23^0C in our measurements. The drops were first formed in one kind of gel under pressure. Then the pressure was released, and the drops were "superheated" (11). The gel is composed of (by weight) 1 part of water, 1 part of glycerine, and 1.25 parts of water soluble Aquasonic 100 ultrasound transmission gel (from Packer Laboratories, Inc., NJ), mixed uniformly and centrifuged to remove gas bubbles. The viscosity of the gel retards the drops's moving, and the smoothness of the gel prevents the drops from vaporizating. In each experiment, one drop thus formed was introduced into the host water with a cluster of the gel. The gel gradually dissolved in water, and then the drop floated up and was trapped by the acoustic field. The amount of the gel going into water with the drop was no more than 0.1 g, which was no more than 0.05% of the amount of host water.

Some experiments were done in order to check if the gel is surface-active. First, we measured the surface tension of water against

air, then put some gel (about 0.2% by volume) into the water and measured the surface tension again after the gel was dissolved in the water. The ring detachment method was used in the measurements. There was no detectable difference in the measured surface tension due to the introduction of gel. Secondly, we did several quadrupole oscillation experiments for hexane and pentane; the host water had gel dissolved in it (about 0.1 % in volume); the test drop was injected into water directly from a syringe. The measured interfacial tension and damping constant showed no difference with other data which were taken with clean host water. Therefore, we judged that the gel is not surface active in water-hexane and water-pentane interfaces: that is, there is no tendency for the gel to pack into or to migrate away from the interface and to change the interfacial tension by any detectable amount.

On the other hand, when we did experiments of hexane and pentane which had the test drops prepared under the same precedure as for surperheated drops, the oscillations of the drops exhibited much greater damping by a factor of 2 to 3. These tests showed significant interfacial viscosity probably due to trace amount of residue of the gel in the interface. This raised the uncertainty of these measured interfacial tensions. The inferred interfacial tension is lower than that for non-contaminated interface: 47.3 dyne/cm for water-hexane, and 45.5 dyne/cm for water-pentane. The coefficient of interfacial dilatational viscosity κ calculated from these data is in the order of

0.01 dyne sec/cm. Thus the interfacial viscous stress is in the order

of 0.1 dyne/cm for the amplitude of oscillations in our measurements.

The inferred interfacial tension was 52 dyne/cm for water-propane,

50 dyne/cm for water-isobutane, and 48 dyne/cm for water-butane. In the

water-propane measurements, the drops dissolved in water gradually, and

the interfacial tension decreased gradually with time presumably due to

the increase of the concentration of propane in water near the

interface. The samples of propane, butane, and isobutane were from

Linde of instrument grade ($99\%^+$).

4.3   Water-hexane-surfactant

Measurements have been made for the interfacial tension between water

and hexane with some surface active agents dissolved in one of the two

phases. With the automatic tracking feature built into our apparatus,

we got the history of the interfacial tension after the drop was

introduced. Fig. 6 shows one example for the history of the interfacial

tension in one measurement. In this measurement, first a hexane drop

was in water without contamination, eight minutes later a little

(≈0.02cc) surfactant (Liqui-nox detergent from Alconox, Inc., N.Y.) was

introduced near the top surface of the water. No change in the

interfacial tension was observed until another 7 minutes later when some

surfactant molecules reached the interface and the interfacial tension

started to decrease. The interfacial tension kept decreasing as more

- 17 -

surfactant molecules packed into the interface and gradually reached

equilibrium after about 100 minutes. Information about the rate of

change of the interfacial density (the number of surfactant molecules on

a unit area of interface) (12) may be able to be deduced from the slope

of the data curve such as in Fig. 6.

Literature data taken with static methods are available regarding

the equilibrium interfacial tension with the presence of surfactants

(e.g. (13), (14), and (15)). We did measurements with common

surfactants, and the final equilibrium interfacial tension are compared

with the literature data as shown in Fig. 7 and 8. Reasonable good

agreement is shown between the data of this work and the literature

data. The measured damping constants were about 50% higher than the

theoretical prediction assuming there is no contamination. The

interfacial viscosity thus can be estimated as in the order of 0.002

dyne•sec/cm.

5. SUMMARY AND CONCLUSIONS

A technique has been developed for measuring interfacial tension.

Acoustic forces are employed to levitate a liquid drop in a liquid host

and to drive the drop into quadrupole shape oscillations. The drop's

oscillation is detected optically. The resonance frequency of the drop

is tracked automatically by the aid of a phase-lock feedback loop. The

frequencies associated with several phase angles near the quadrupole

resonance of the drop are measured, as is the diameter of the drop.

These measurements allow the interfacial tension to be calculated given the densities of both the drop and the host liquids.

Though the basic idea is similar to the traditional oscillating drops method, this technique has its distinct features which provide some special advantages. Because the drop can be levitated almost indefinitely, good measurements can be made with comparative ease. Because the drop comes in contact only with the host liquid, which behaves as a very smooth and clean container, the drop can be in a metastable state. Because of the long life time of the drop and because of the tracking feature, any changes of the interfacial tension can be monitored automatically.

This technique has been applied to different interfaces such as water-hexane, water-propane, and water-hexane-surfactant, and the results are reported. Comparison is made with the literature data when they are available, and good agreement is shown. The propane samples in the experiments were superheated by 65 Celsius degrees. condition. One example of the data showed the history of the interfacial tension after one hexane drop was introduced into water; the interfacial tension changed over 60% during two hours owing to the addition of some surfactant. The coefficient of dilatational interfacial viscosity is estimated for the contaminated interfaces based on the damping measurement of the oscillations.

This technique provides a way to measure interfacial tension especially for some situations where traditional methods are non-applicable. It also provides some new information about interfaces. It should be a useful tool for experimental study of interfaces.

ACKNOWLEDGMENTS

REFERENCES

1. Jasper, J.J., in "Treatise on Analytical Chemistry", ed. Kolthoff, I.M., and Elving, P.J., part 1, vol. 7, chap. 82, John Wiley & Sons, New York, 1967.

2. Apfel, R.E., J. Acoust. Soc. Am., 59(2), pp. 339-343, 1976.

3. Marston, P.L., J. Acoust. Soc. Am., 67(1), pp. 15-26, 1980.

4. Hsu, C.J., and Apfel, R.E., submitted to J. Fluid Mec., 1984.

5. Lamb, H, "Hydrodynamics" sect. 275, 355, Dover, New York, 1945.

6. Hsu, C.J., Ph.D. thesis, Yale University, Dec. 1983.

7. Miller, C.A., and Scriven, L.E., J. Fluid Mech., vol. 32, part 3, pp. 417-435, 1968.

8. Marston, P.L., and Apfel, R.E., J. Acoust. Soc. Am., 67(1), pp. 27-37, 1980.

9. Chu, B.T., and Apfel, R.E., J. Acoust. Soc. Am., Vol. 72, No. 6., 1982.

10 Trinh, E., Zwern, A., and Wang, T.G., J. Fluid Mech., vol. 115, pp. 453-474, 1982.

11. Apfel, R.E., U.S. pat. 4, 143, 274.

12. Motomura, K., J. Colloid Interface Sci., 64, 348 (1978).

13 Motomura, K., et. al., J. Colloid Interface Sci., 64, 356 (1978).

14 Motomura, K., et. al., J. Colloid Interface Sci., 67, 247 (1978).
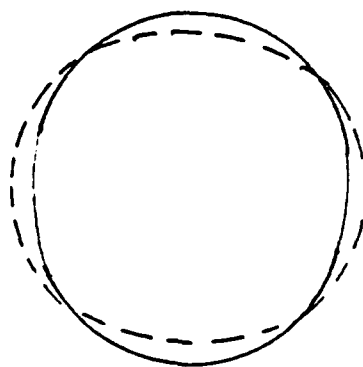
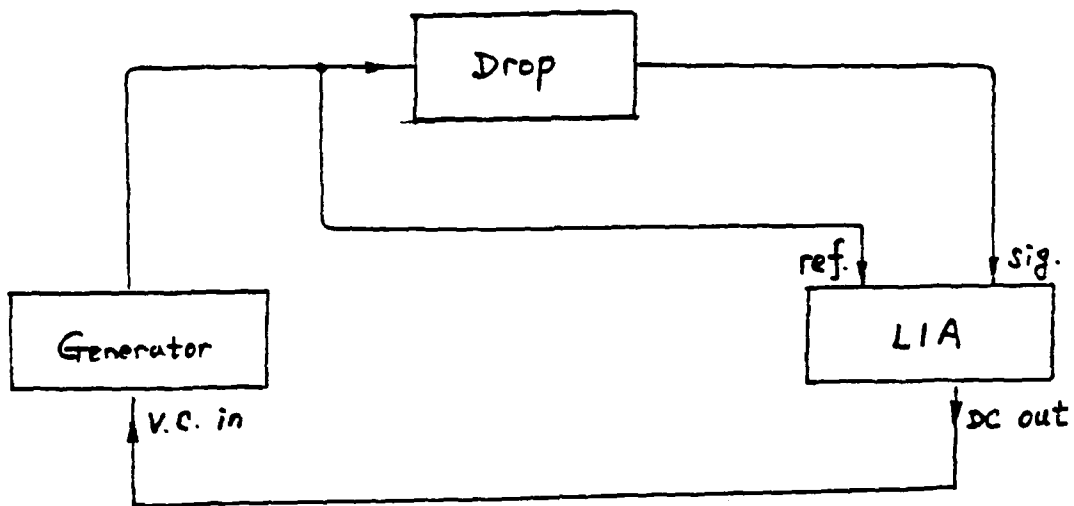15. Rehfeld, S.J., J. Phys. Chemistry, 71(3), 738 (1967).

figure 1.
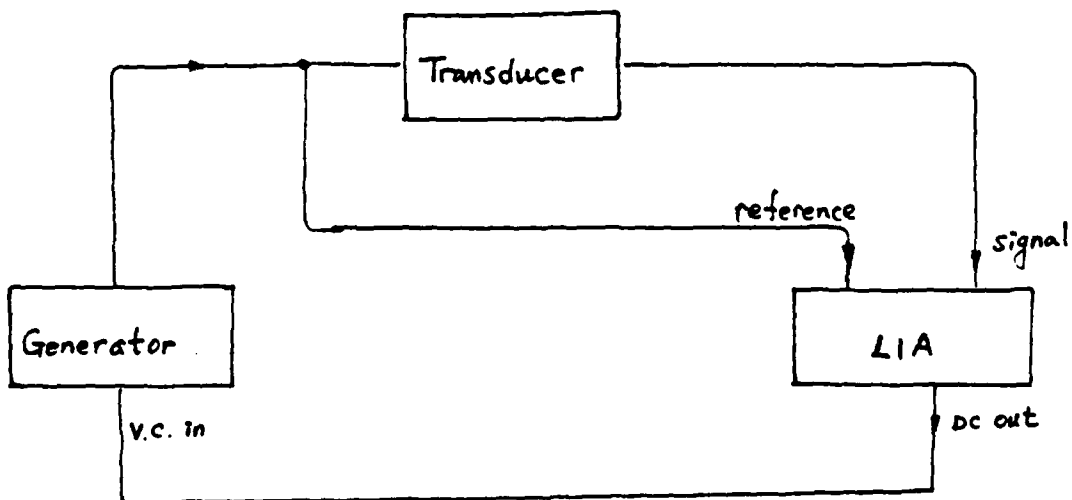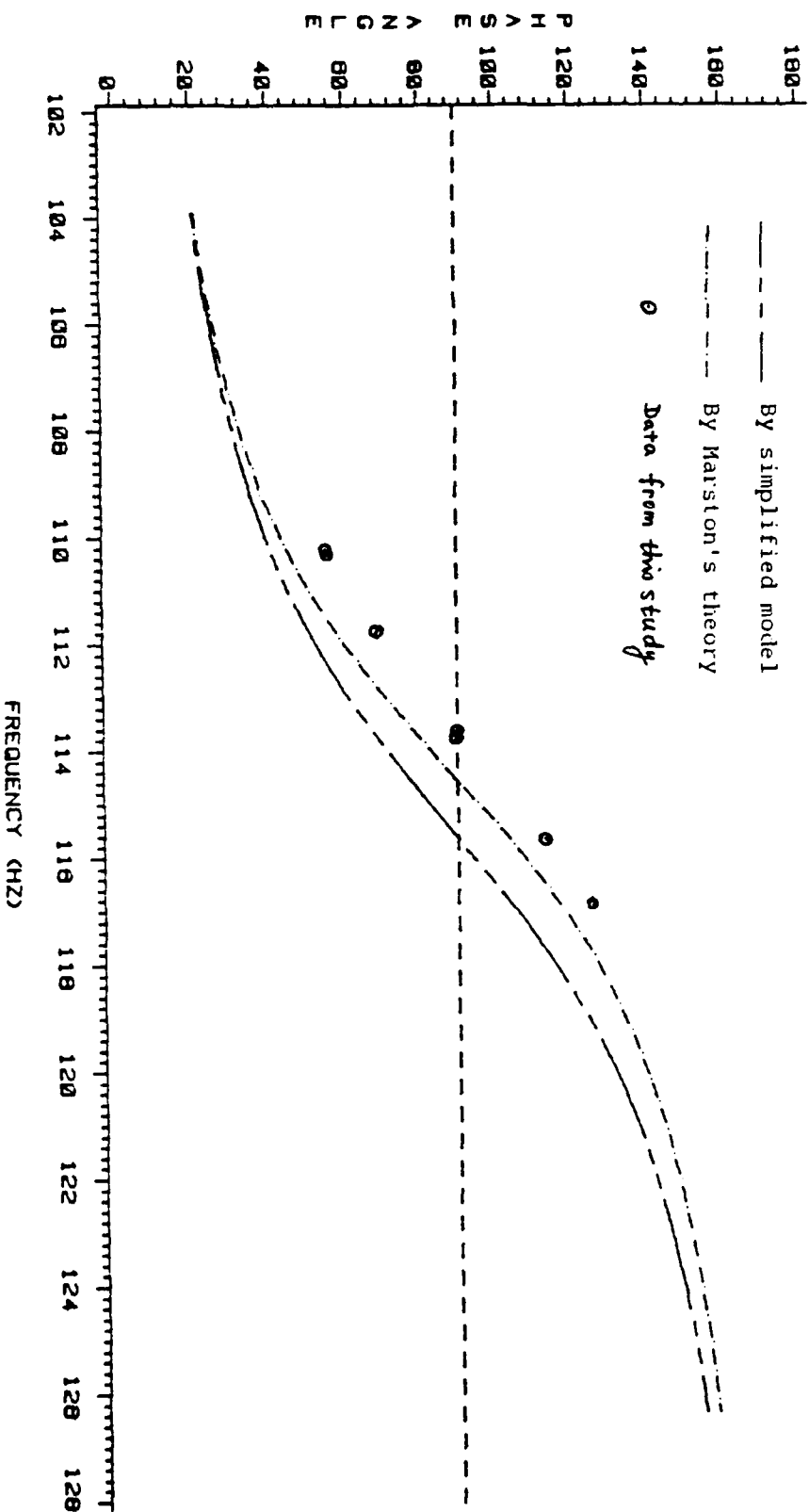
figure 2.

figure 3.

figure 4.

Figure 5. Phase vs. frequency curves given by the simplified model and Marston's theory respectively: Example for host, water; drop, hexane; drop radius, 0.0825 cm.
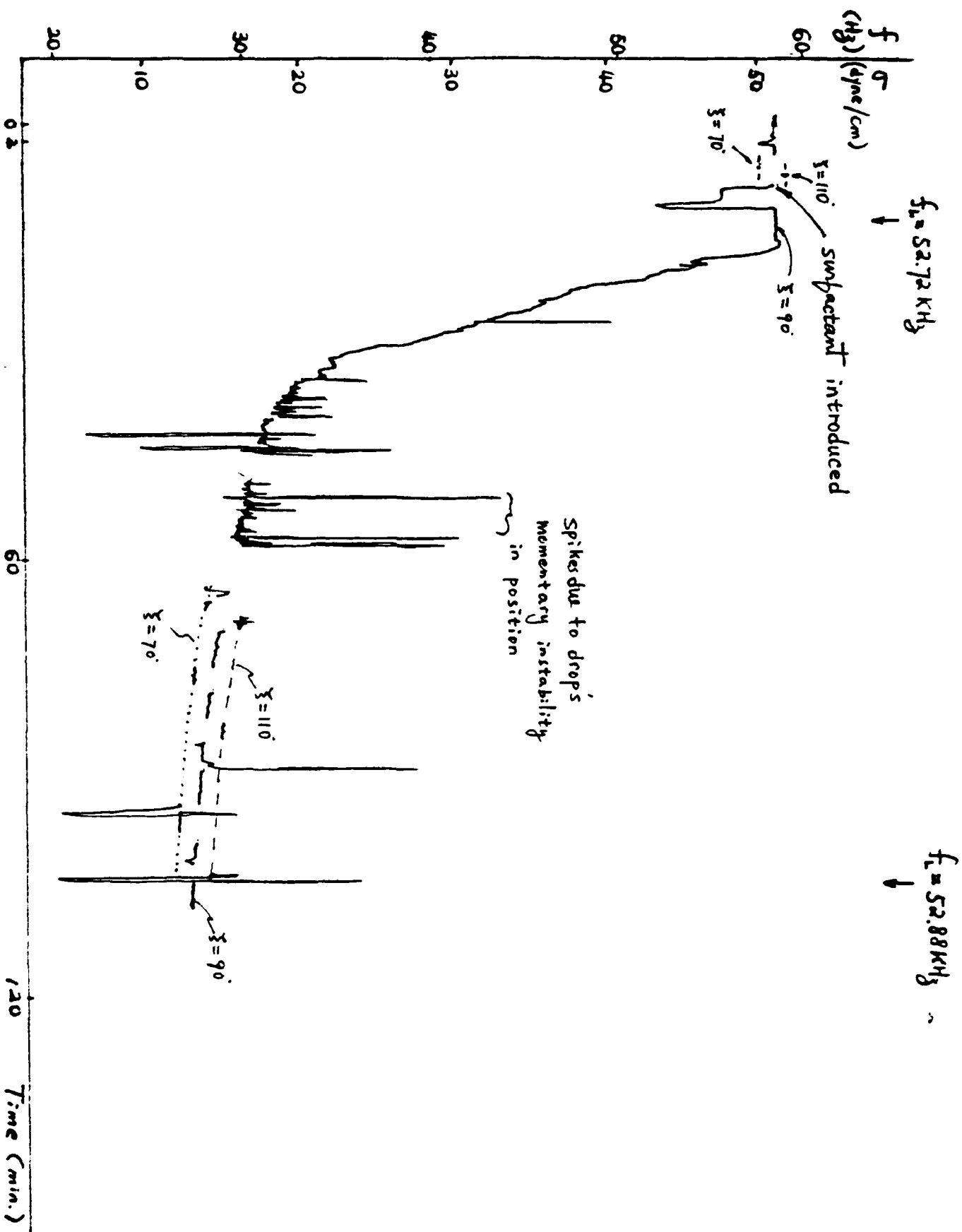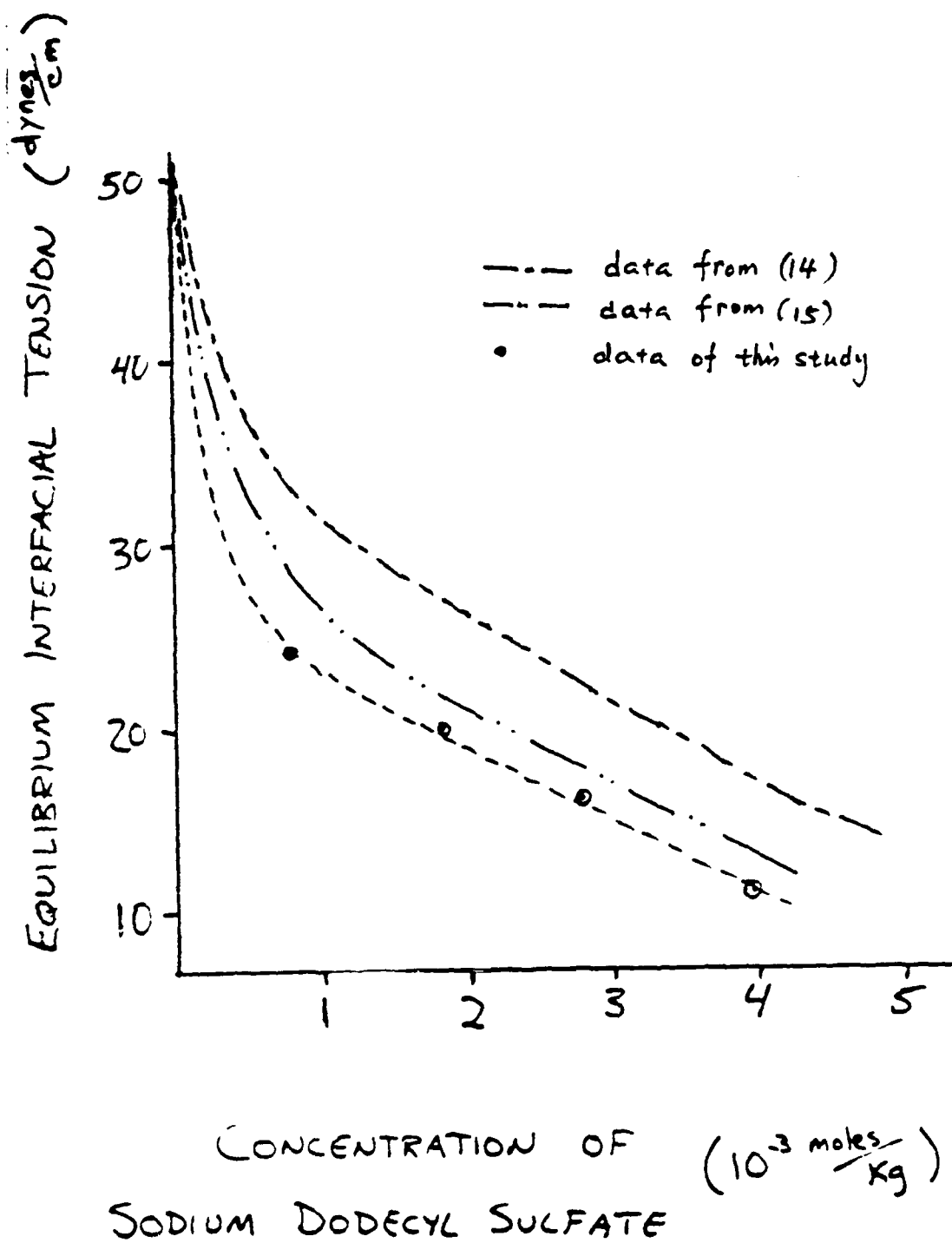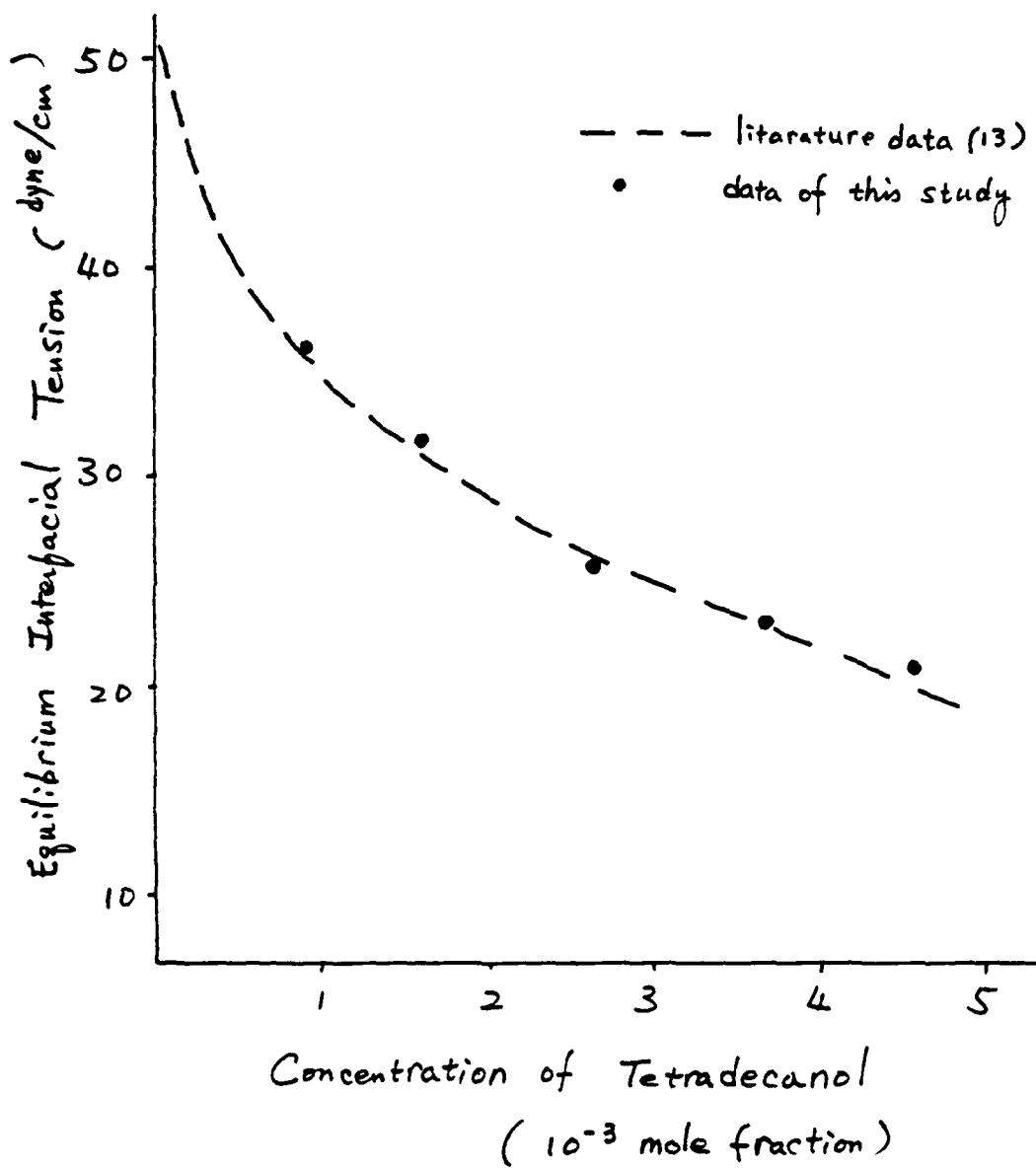
By simplified model

By Marston's theory

Data from this study

PHASE ANGLE

FREQUENCY (HZ)

figure 6.

figure 7.

figure 8.

END

FILMED

3-85

DTIC